LBL-18766 c.2
Preprint

Lawrence Berkeley Laboratory

UNIVERSITY OF CALIFORNIA

RECEIVED
LAWRENCE
BERKELEY LABORATORY

MAR 26 1985

LIBRARY AND
DOCUMENTS SECTION

Materials & Molecular Research Division

Submitted to Chemical Engineering Science

PHOTOELECTROCHEMICAL DEVICES FOR
SOLAR ENERGY CONVERSION

M.E. Orazem and J. Newman

January 1985

TWO-WEEK LOAN COPY

This is a Library Circulating Copy which may be borrowed for two weeks.

LBL-18766 c.2

Prepared for the U.S. Department of Energy under Contract DE-AC03-76SF00098

DISCLAIMER

This document was prepared as an account of work sponsored by the United States Government. While this document is believed to contain correct information, neither the United States Government nor any agency thereof, nor the Regents of the University of California, nor any of their employees, makes any warranty, express or implied, or assumes any legal responsibility for the accuracy, completeness, or usefulness of any information, apparatus, product, or process disclosed, or represents that its use would not infringe privately owned rights. Reference herein to any specific commercial product, process, or service by its trade name, trademark, manufacturer, or otherwise, does not necessarily constitute or imply its endorsement, recommendation, or favoring by the United States Government or any agency thereof, or the Regents of the University of California. The views and opinions of authors expressed herein do not necessarily state or reflect those of the United States Government or any agency thereof or the Regents of the University of California.

LBL-18766

Photoelectrochemical Devices for Solar Energy Conversion

Mark E. Orazem

Department of Chemical Engineering
Thornton Hall
University of Virginia
Charlottesville, Virginia 22901

and John Newman

Materials and Molecular Research Division
Lawrence Berkeley Laboratory
and
Department of Chemical Engineering
University of California
Berkeley, California 94720

January, 1985

This work was supported by the Assistant Secretary for Conservation and Renewable Energy, Office of Energy Systems Research, Energy Storage Division of the U.S. Department of Energy under Contract Number DE-AC03-76SF00098.

Photoelectrochemical cells are distinguished by the use of a semiconductor-electrolyte interface to create the necessary junction for use as a photovoltaic device.[B1-2,F9,M2,E1,G8] This article presents a description of this device from an electrochemical engineering viewpoint. The traditional chemical engineering fundamentals of transport phenomena, reaction kinetics, thermodynamics, and system design provide a useful foundation for the study of semiconducting devices. The motivation for the study of photoelectrochemical cells is discussed, and a physical description of the cell features is presented. This leads to a tutorial on the mechanism of cell operation, including descriptions of the phenomena of band-bending and straightening, the effect of interfacial phenomena, and current flow. Mathematical relationships are developed which describe this system, and the influence of cell design is discussed.

Many review papers cover the physics and chemistry of photoelectrochemical cells (see, e.g., references G13, G3, A8, R2, H4, N9, T3, W10, M13, M21, and K9). This review is distinguished by an emphasis on quantitative design and optimization of large-scale photoelectrochemical cells and by a mathematical description that accounts for the influence of the nonideal behavior associated with large electron and hole concentrations in the semiconductor. This review also provides a contrast between a physical description of electrons in terms of energies and statistical distributions and a chemical description in terms of concentrations and activity coefficients.

1. Semiconductor Electrodes

Semiconductors are characterized by the difference in energy between valence and conduction-band electrons. Electrons can be transferred from the valence band to the conduction band by absorption of a photon with energy greater than or equal to the transition or band-gap energy. When the electron moves into the higher energy level, it leaves behind a vacancy in the valence band, or hole. Both the negatively charged electrons and the positively charged holes are mobile and can serve as charge carriers (see, e.g., references G14, O2, S17, H3, or I2). In the presence of a potential gradient (or electric field), electrons and holes tend to migrate in opposite directions and can result in a net flow of electrical current. In the absence

of a potential gradient, electron-hole pairs produced by illumination recombine with no net flow of electrical current. Photovoltaic devices therefore require an equilibrium potential gradient in the illuminated region of the semiconductor.

A potential gradient can be created by forming an interface or junction with a semiconducting material. Metal-semiconductor, p-n semiconductor, and semiconductor-electrolyte interfaces have been used in the construction of photovoltaic cells.[H15-16,W1] The interface in a p-n junction photovoltaic cell can be constructed by doping the surface of an n or p-type semiconductor with atoms that invert the semiconductor type. These atoms are then thermally diffused into the host semiconductor to an optimal depth. Diffusion rates in grain boundaries greatly exceed those in the bulk crystal; thus the need for a distinct boundary limits this technique to single-crystal host semiconductors. The junction between an electrolyte and a semiconductor, in contrast to the thermally-diffused p-n junction, is formed spontaneously when the semiconductor is immersed in the electrolyte. The doping and diffusion processes are not needed, and polycrystalline semiconductors can be used.[H10] Vapor or plasma deposition of thin metallic or semiconducting films also allows construction of solar cells with polycrystalline materials. These solid-state-junction photovoltaic devices have the advantages attributed to photoelectrochemical cells and avoid the associated corrosion problems.[M18]

1.1 Physical Description

The principal elements of the liquid-junction photovoltaic cell, as shown in Figure 1, are the counterelectrode, the electrolyte, the semiconductor-electrolyte interface, and the semiconductor. The distribution of charged species (ionic species in the electrolyte and electrons and holes in the semiconductor) is altered by the semiconductor-electrolyte interface, and an equilibrium potential gradient is formed in the semiconductor. The interfacial region may be associated with adsorption of charged species or with surface sites. The charge is distributed such that the interface taken as a whole is still electrically neutral. Sunlight is absorbed within the semiconductor and causes generation of electron-hole pairs which are separated by the potential gradient. This separation leads to concentration and potential driving forces for electrochemical reactions at the semiconductor-electrolyte interface. The electrochemical reactions allow passage of

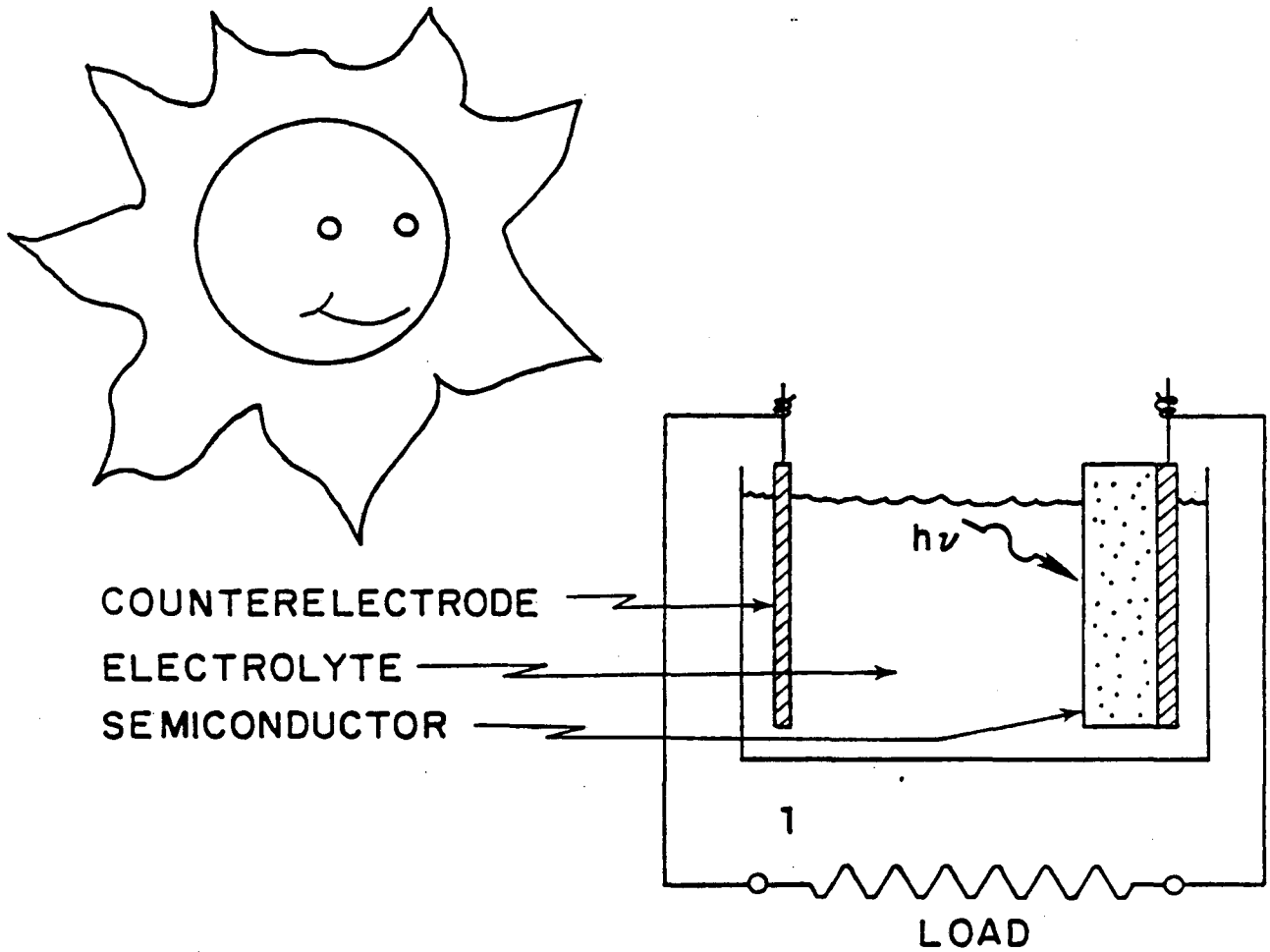

Figure 1. The photoelectrochemical cell.

electrical current through the cell.

The semiconductor and the electrolyte phases are conveniently characterized through macroscopic relations. A microscopic model is required for the interface between the bulk phases. This model can be arbitrarily complex but is restricted by the requirement that thermodynamic relationships among the bulk phases hold. A convenient model for the interfacial region is represented in Figure 2. The interface is represented by four planes, inner and outer Helmholtz planes on the electrolyte side of the interface and inner and outer surface states on the semiconductor side. The outer Helmholtz plane (OHP) is the plane of closest approach for (hydrated) ions associated with the bulk solution. The inner Helmhotz plane (IHP) passes through the center of ions specifically adsorbed on the semiconductor surface. The outer surface state (OSS) represents the plane of closest approach for electrons (and holes) associated with the bulk of the semiconductor. The inner surface state (ISS) is a plane of surface sites for adsorbed electrons. If surface sites are neglected, the ISS and the OSS are coincident.

This model of the semiconductor-electrolyte interface is an extension of the classical Gouy-Chapman diffuse-double-layer theory.[G12,D11,S13,N4] Charge adsorbed onto the IHP and the ISS planes is balanced by charge in the diffuse region of the electrolyte and the space-charge region of the semiconductor. The net charge of the interface, including surface planes and diffuse and space-charge regions, is equal to zero. Within a given model, reactions may be written to relate concentrations and potentials at interfacial planes. Interfacial sites or energy levels for electrons or holes can be included at the ISS. Interfacial reactions may thus include adsorption of ionic species from the OHP to the IHP, adsorption of electrons from the OSS to sites of specified energy at the ISS, surface recombination through ISS sites, and direct surface recombination. Emission of electrons from the semiconductor may take place by electron transfer from surface sites at the ISS to adsorbed ions (trapping and subsequent emission), transfer of OSS electrons to adsorbed ions (thermionic emission), transfer of electrons in the space charge region to adsorbed ions (thermally enhanced field emission or direct tunneling), transfer of electrons in the neutral region to adsorbed ions (field emission or direct tunneling), and transfer of electrons in the neutral region to adsorbed ions through defects in the bulk (multistep tunneling). Such

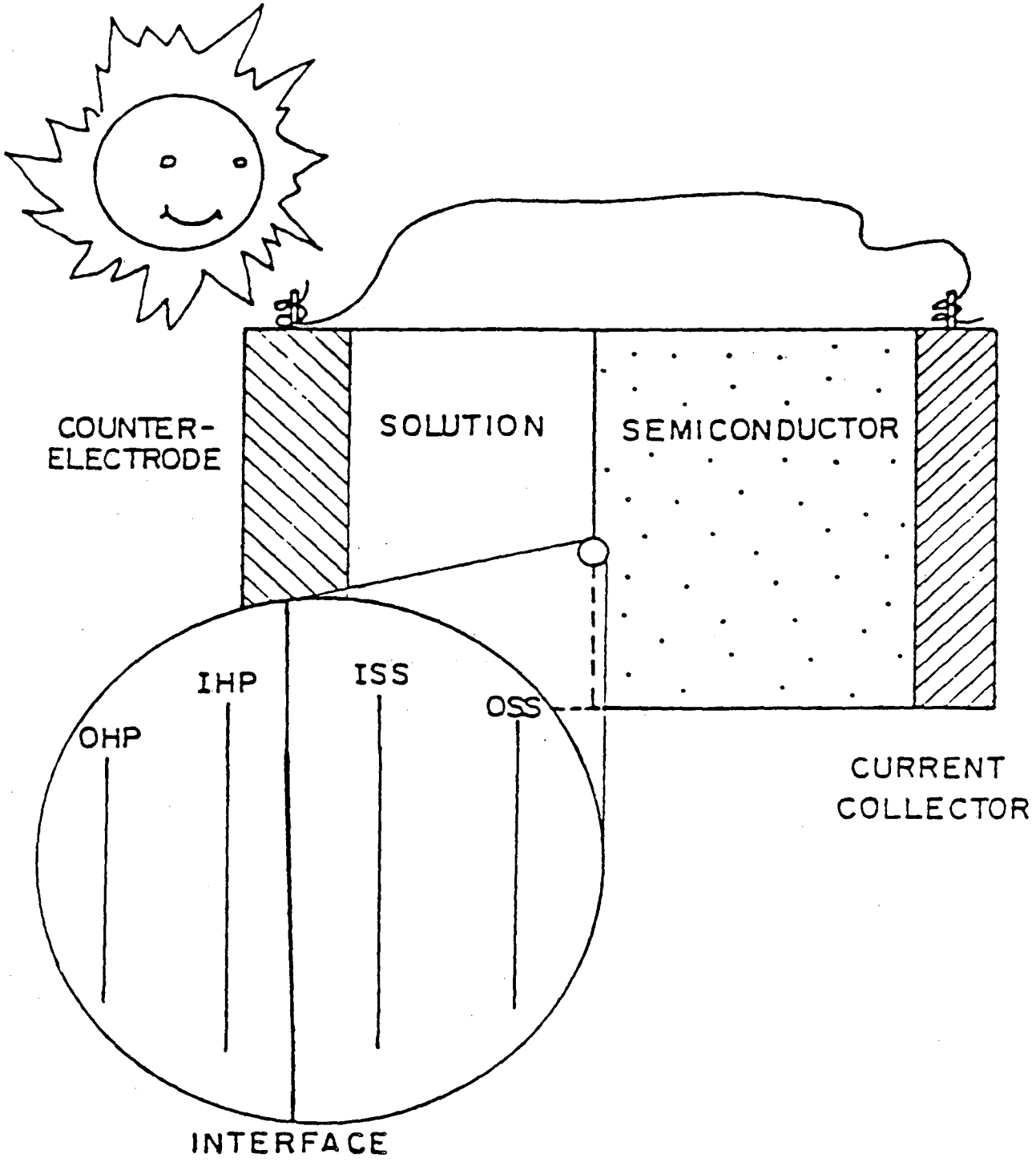

Figure 2. Physical model of the semiconductor-electrolyte interface in a photoelectrochemical cell.

reactions may also involve ions associated with the OSS or with the diffuse part of the double layer. These reactions may also take place in the reverse direction. These reaction mechanisms are also described by Fonash.[F5]

1.2 The Mechanism of Cell Operation

Formation of an interface perturbs the potential distribution in the semiconductor, and this perturbation creates the junction necessary for the photovoltaic effect in solar cells. Examination of the potential distribution in the liquid-junction cell therefore provides insight into the forces driving the cell. The following discussion is based on the numerical solution of the equations governing a GaAs photoanode with a selenium redox couple.[O3,O5-7] The governing equations are presented in section 2. Interfacial reactions were included but were assumed to be sufficiently fast that the operation of the cell was limited by the transport and generation of electrons and holes in the semiconductor. The potential distribution is presented in Figure 3. In the dark, at open-circuit, (curve a) the system is equilibrated. The potential is nearly constant throughout the solution and the interfacial planes (OHP, IHP, ISS, and OSS). The potential varies in the semiconductor in response to charge distributed in the semiconductor. This variation of electrical potential in the equilibrated semiconductor is termed **band-bending**. The difference in potential between the semiconductor-electrolyte interface and the current collector-semiconductor interface of the semiconductor is the **flat-band potential**. This is the potential that would need to be applied in order to achieve uniform potential in the semiconductor.

Under illumination at open circuit (curve b) the concentrations of electrons and holes increase, and the variation of potential in the semiconductor decreases. The decrease in potential variation in response to illumination is referred to as the **straightening of the bands**. The charges of holes and electrons, generated by the illumination, tend to go in opposite directions under the influence of the electric field. Their accumulation, at open circuit, at various locations creates an electric field which tends to cancel that existing in the dark and leads to this straightening of the bands. The difference between the potential in the dark and under illumination represents a driving force for flow of electrical current. The potential distribution near the short-circuit condition (curve c) approaches the equilbrium distribution. Short-circuit is defined as the condition of a zero

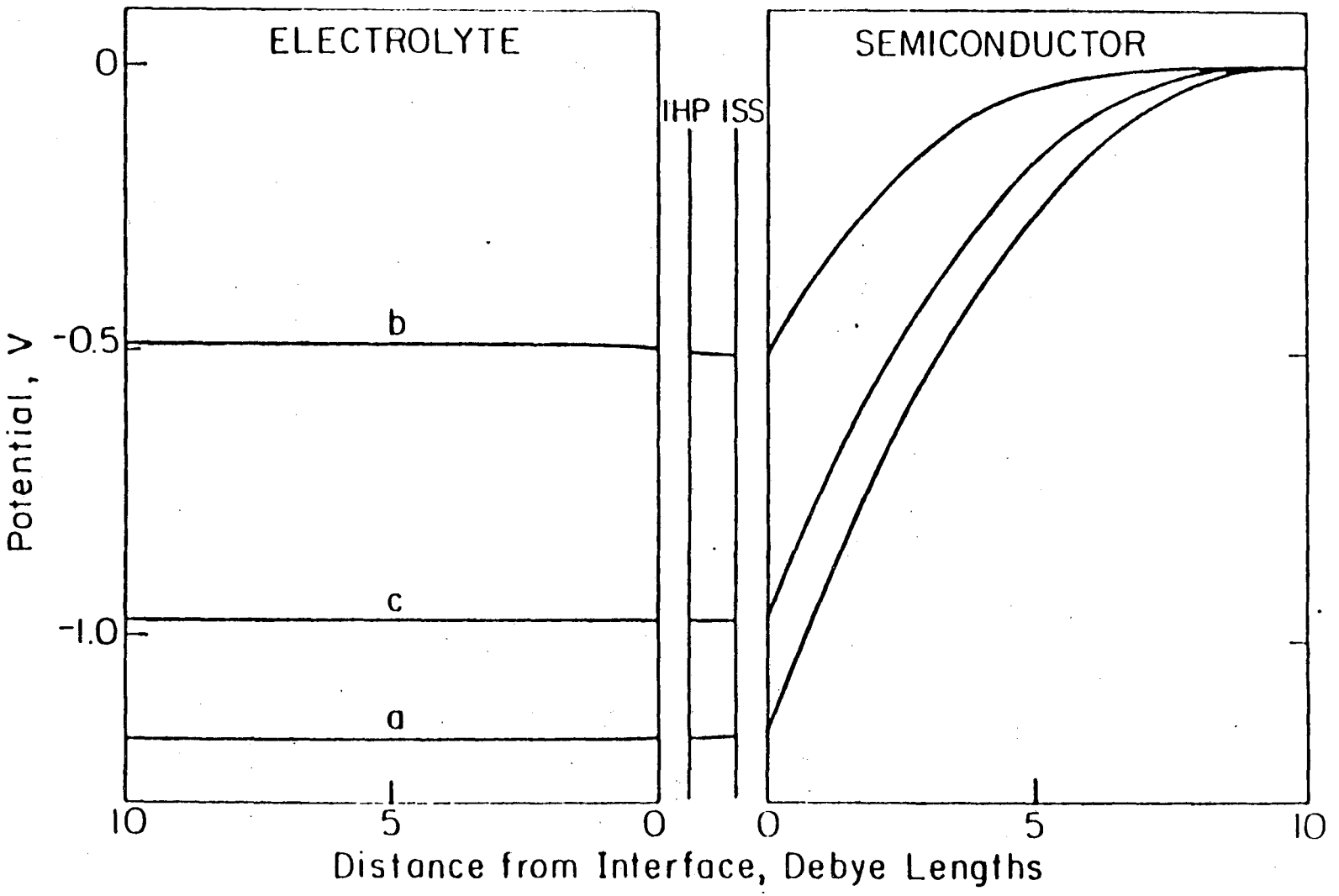

Figure 3. Potential distribution for the photoelectrochemical cell with no interfacial kinetic limitations. Curve a, open circuit in the dark; curve b, open circuit under 882 W/m^2 illumination; and curve c, near short circuit ($\underline{i}$ = -23.1 mA/cm^2) under illumination.

cell potential. The description presented here neglects the influence of electrolyte resistance and counterelectrode kinetic and mass-transfer limitations in determining the condition of short-circuit. The inclusion of these effects cause the short-circuit potential distributions described here to occur at negative cell potentials. All the variation in potential (from open circuit in the dark to open circuit under illumination to short-circuit under illumination) takes place in the semiconductor. The potential drop across interfacial planes is comparatively small and invariant.

Concentration distributions of holes and electrons in the semiconductor are presented in Figure 4 for a system with no interfacial kinetic limitations. Under equilibrium conditions the concentration of holes (curve a) is essentially zero in the bulk of the semiconductor and increases near the negatively charged interface. Conduction electrons are depleted near the interface and reach a value of 0.328 dimensionless units at the current collector, where the concentrations are scaled by the dopant concentration (N_d-N_a), and N_d and N_a represent the concentrations of ionized electron donors and acceptors, respectively. The electron concentration in a neutral region of the semiconductor would have a value essentially equal to 1.0. The equilibrated semiconductor of Figure 4 can therefore be described as having an inversion region extending from the semiconductor-electrolyte interface to 0.5 Debye lengths from the interface and a depletion region extending to the current collector. An inversion region is usually defined as the region for which the dimensionless minority carrier concentration is greater than one. The definition used here is for a region where the minority carrier concentration cannot be assumed to be negligible or is greater than the majority carrier concentration.

The semiconductor described by Figure 4 has a net positive charge which is balanced by charge associated with the diffuse region of the electrolyte and with the interface such that system electroneutrality is maintained. The potential gradient, the driving force for migration of charged species, is balanced by the concentration gradient, which drives diffusion. Thus, the net flux of each species in the semiconductor is equal to zero at equilibrium.

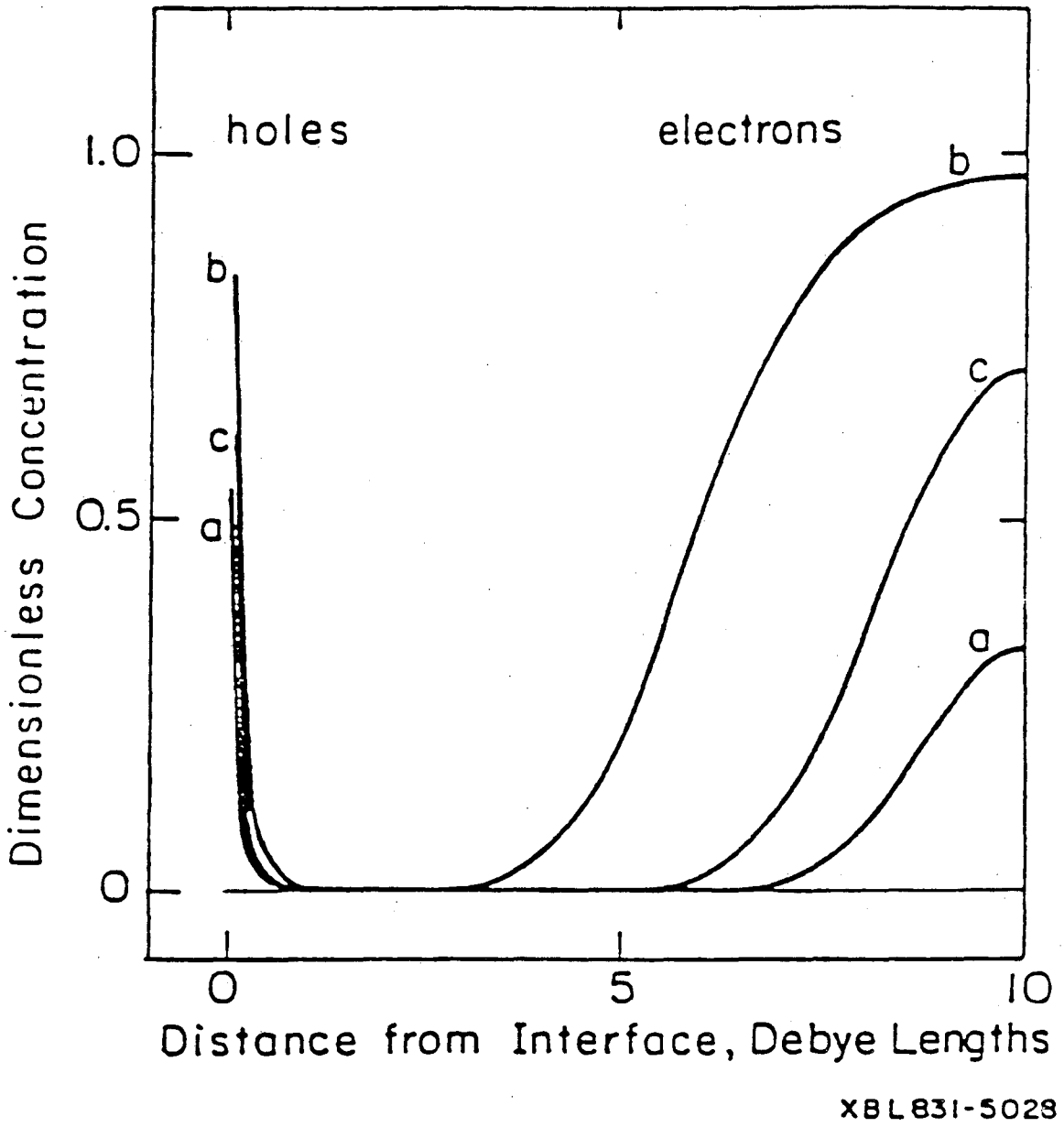

Figure 4. Concentration distribution for the photoelectrochemical cell with no interfacial kinetic limitations. Curve a, open circuit in the dark; curve b, open circuit under 882 W/m^2 illumination; and curve c, near short circuit ($\underline{i}$ = -23.1 mA/cm^2) under illumination. Concentrations are dimensionalized by the net dopant concentration $N_d - N_a$.

Illumination under open-circuit conditions produces electron-hole pairs, which are separated by the potential gradient (see Figure 3). The concentration of holes increases near the interface, and the concentration of electrons increases near the current collector (curve b in Figure 4). Under steady-state conditions, the rate of generation of electron-hole pairs is balanced by the rate of homogeneous and interfacial recombination. As the system without kinetic limitations approaches short circuit (curve c in Figure 4), the concentrations of holes and electrons approach the equilibrium distributions.

The potential and concentration distributions described for the system with no kinetic limitations to interfacial reactions are constrained by the rates of generation and mass transfer in the semiconductor. More generally, kinetic limitations to interfacial reactions are compensated by the increased interfacial potential and concentration driving forces required to allow passage of electrical current. The presence of these limitations may be inferred from experimental data by inflection points in the current-potential curve.

2. Mathematical Description

Macroscopic transport equations are commonly used to describe the semiconductor and the electyrolyte in the liquid-junction cell. A microscopic model of the semiconductor-electrolyte interface couples the equations governing the macroscopic systems.

2.1 Semiconductor

The electrochemical potential of a given species can arbitrarily be separated into terms representing a reference state, a chemical contribution, and an electrical contribution.

$$\mu_i = \mu_i^\theta + RT\ln(c_i f_i) + z_i F\Phi \ , \qquad (1)$$

where Φ is a potential which characterizes the electrical state of the phase and can be arbitrarily defined. The potential used here is the electrostatic potential which is obtained through integration of Poisson's equation.[P6] Equation (1) can be viewed as the defining equation for the activity

coefficient, f_i.

The flux density of an individual species within the semiconductor is driven by a gradient of electrochemical potential;

$$\underline{N}_i = -c_i u_i \nabla \mu_i \quad . \tag{2}$$

This can be written for electrons and holes in terms of concentration and potential gradients (see, e.g., references G3 or N4). The flux density of holes $\underline{N}_h$ is therefore given by

$$f_h \underline{N}_h = -u_h RT \nabla (p f_h) - u_h (p f_h) F \nabla \Phi \quad , \tag{3a}$$

and the flux density of electrons $\underline{N}_e$ by

$$f_e \underline{N}_e = -u_e RT \nabla (n f_e) + u_e (n f_e) F \nabla \Phi \quad . \tag{3b}$$

The concentrations of electrons and holes are represented by n and p, respectively, and the mobilities u_i are related to the diffusivities D_i by the Nernst-Einstein equation

$$D_i = RTu_i \quad . \tag{4}$$

This equation is appropriate for both dilute and concentrated solutions.[N4] Nonidealities associated with more concentrated solutions are incorporated within the activity coefficient.

Equation (3) can be simplified through the assumption of constant activity coefficients. Under the assumption of constant activity coefficients, equation (3) is in harmony with a Boltzmann distribution of electrons and holes. Such an approach is valid for p/N_v and n/N_c less than 0.1. Expressions have been presented for the activity coefficients of electrons and holes.[R11,P2-3,H17,G16] The use of concentration-dependent activity coefficients, e.g.,

$$f_h = \frac{1}{1 - p/N_v} \tag{5a}$$

for holes and

$$f_e = \frac{1}{1 - n/N_c} \tag{5b}$$

for electrons,[O9] extends the validity of the transport equations to

dimensionless concentrations less than 1. The expressions given in equation (5) are thermodynamically consistent, are valid in regions of charge, and are consistent with a Fermi-Dirac distribution for electrons. These expressions do not, however, account for band-perturbing and band-gap narrowing effects associated with heavily-doped semiconductors. The activity coefficients can be modified to account for these effects, but this modification requires more information on the energy-band structure (see references L6, D2, R11, L12, and H5). Inclusion of activity coefficients is necessary for highly-doped semiconductors and for semiconductors subjected to a large electric field.

Another approach toward characterization of degenerate semiconductors has been to include the nonidealities associated with degeneracy within a modified Nernst-Einstein relationship.[L4,L17,M5,K12] The modified Nernst-Einstein relationship is given by[L3]

$$D_i = RTu_i \frac{F_{1/2}(\eta)}{\frac{\partial}{\partial \eta} F_{1/2}(\eta)} , \tag{6}$$

where $F_{1/2}(\eta)$ is a tabulated integral[S2,A10] and η is proportional to the difference between the electrochemical potential of the species i and the respective band-edge energy. This approach is related to the activity coefficient used in the above development by[L5]

$$\frac{F_{1/2}(\eta)}{\frac{\partial}{\partial \eta} F_{1/2}(\eta)} = \left(1 - \frac{d\ln f_i}{d\ln c_i} \right) . \tag{7}$$

The validity of the Nernst-Einstein relation rests on the fact that the driving force for both migration and diffusion is the gradient of the electrochemical potential, and the decomposition of this into chemical and electrical contributions is arbitrary and without basic physical significance.[G15] Correction of the Nernst-Einstein relationship to account for nonideal behavior represents a decomposition of the electrochemical potential gradient such that the diffusional flux density is proportional to the gradient of concentration, not activity as given in equation (3). The advantages of the approach represented by equations (1) through (5) are that the influence of nonideal behavior is separated from transport properties and

that only one transport property need be measured for each species. Furthermore, the transport property can be expected to be a weaker function of concentration. The activity coefficients presented in equation (5) can also be employed within the framework of the transport theory for concentrated solutions.[N4,B5]

Homogeneous reaction takes place in the semiconductor; thus a material balance for a given species, say holes, yields

$$\nabla \cdot \underline{N}_h = R_h, \tag{8}$$

where R_h is the net rate of production of holes under steady-state conditions. The development presented here, while applicable to p-type semiconductors, is oriented toward analysis of an n-type semiconductor in which holes are the minority carrier. Material balances of holes and electrons are not independent, and conservation of the minority carrier was chosen to improve the numerical computational accuracy.

The rate of production of holes is, by stoichiometry, equal to the rate of production of electrons and is governed by three concurrent processes: generation by absorption of light, generation by absorption of heat, and recombination of electrons and holes (i.e., transfer of an electron from the conduction band to the valence band).

$$R_h = G_L + G_{th} - R_{rec} \ . \tag{9}$$

Mathematical models of the homogeneous recombination process have been developed which incorporate single-step electron transfer from one energy level to another. They differ in the assumption of the presence or absence of impurities which allow electrons to have energies between the conduction and valence-band energies.[S11,S4,M19]

Band-to-band kinetic models (presented in Figure 5) allow electrons to have only valence or conduction-band energies. Absorption of the appropriate amount of thermal or electromagnetic energy creates an electron-hole pair; recombination of an electron and a hole releases energy in the form of heat or light. The band-to-band model yields

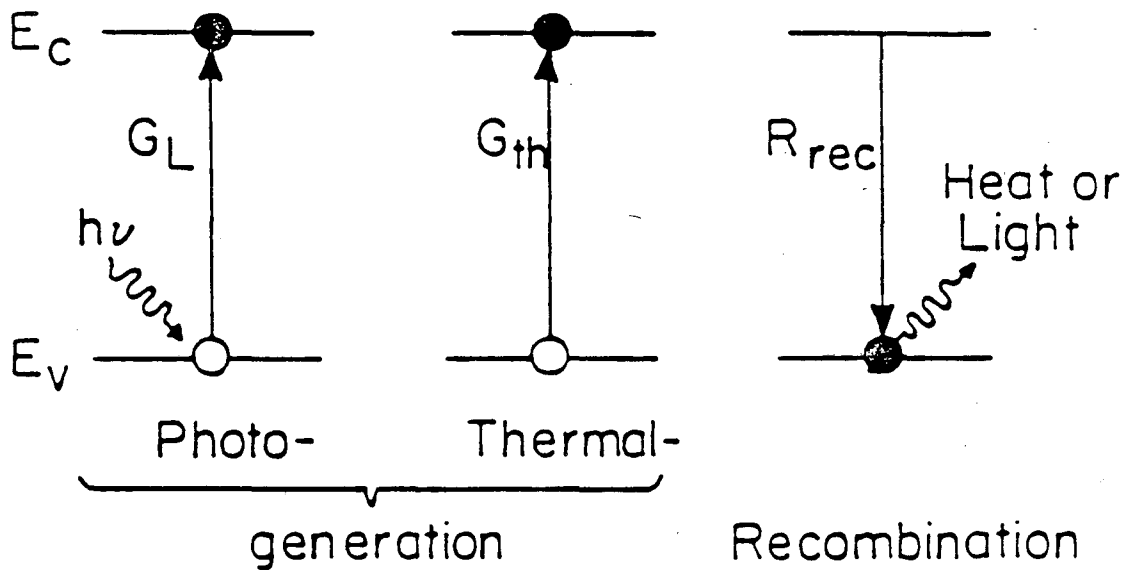

Individual Reaction Rates

$$G_L = \epsilon m q_0 e^{-mx}$$

$$G_{th} = k_{th}(N_c - n)(N_v - p)$$

$$R_{rec} = k_{rec}\, np$$

XBL 831-5023

Figure 5. Schematic representation of band-to-band recombination kinetics in the semiconductor.

$$R_h = \eta m q_o e^{-my} - k_{rec}(np - n_i^2) \quad , \tag{10}$$

where η is the fraction of incident photons with energy greater than the band gap energy, m is the absorption coefficient, q_o is the incident solar flux, and n_i is the intrinsic concentration,

$$n_i = \left(\frac{k_{th}(N_c-n)(N_v-p)}{k_{rec}} \right)^{1/2} \quad . \tag{11}$$

The intrinsic concentration is written in terms of N_c and N_v, the number of available conduction and valence-band sites respectively, and k_{th} and k_{rec}, thermal generation and recombination rate constants. Under equilibrium conditions, the rate of thermal generation is equal to the rate of recombination, and $np = n_i^2$.

Most semiconducting materials contain within their lattice structure impurities or imperfections which may be described as fixed sites with valence-band electron energies within the semiconductor band gap. The trap-kinetics model allows recombination to occur through these sites (see Figure 6). Absorbed radiation drives an electron from the valence band to the conduction band, and all recombination and thermal generation reactions are assumed to occur through trap sites. This model results in

$$R_h = \eta m q_o e^{-my} - \frac{N_t k_2 (np-n_i^2)}{\dfrac{k_1(N_v-p)+k_3(N_c-n)}{k_4} + \dfrac{k_2}{k_4} p + n} \quad , \tag{12}$$

where k_1, k_2, k_3, and k_4 are the rate constants for the corresponding reactions shown in Figure 6. The intrinsic concentration is given by

$$n_i = \left(\frac{k_1 k_3 (N_c-n)(N_v-p)}{k_2 \; k_4} \right)^{1/2} \quad . \tag{13}$$

The expressions for the intrinsic concentration (equations (11) and (13)) are consistent with the expression derived through statistical-mechanical models, e.g.,

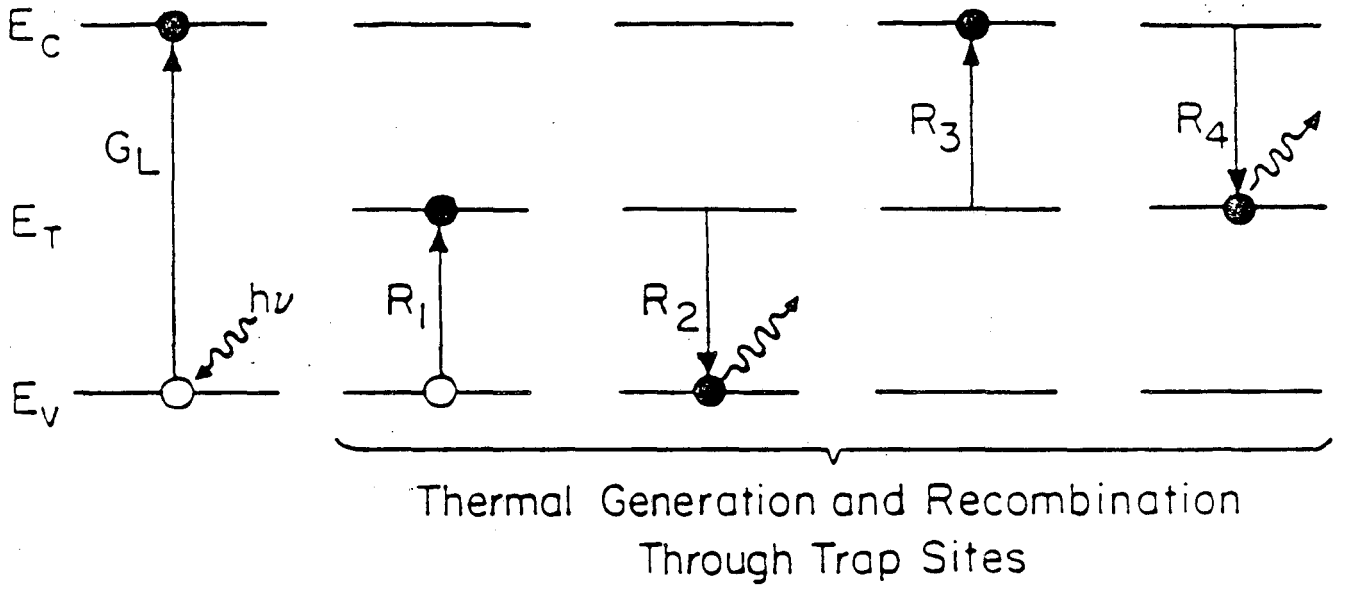

Individual Reaction Rates

$$G_L = \epsilon m q_0 e^{-mx}$$

$$R_1 = k_1(N_V - p)(N_T - n_T)$$

$$R_2 = k_2 n_T p$$

$$R_3 = k_3 n_T (N_C - n)$$

$$R_4 = k_4 n (N_T - n_T)$$

XBL 831-5024

Figure 6. Schematic representation of single-trap recombination kinetics in the semiconductor.

$$np = n_i^2 = (N_c - n)(N_v - p)e^{-E_g/RT} \quad .$$

The intrinsic concentration can be considered to be a constant for a given semiconductor only if the ratios n/N_c and p/N_v are negligibly small compared to unity. The intrinsic concentration is related to the nondegenerate limit n_{lim} and the activity coefficients of equation (5) by

$$n_i = n_{lim} \left(\frac{1}{f_e f_h} \right)^{1/2} \tag{15}$$

The assumption of a constant intrinsic concentration is consistent with the assumption of unity activity coefficients for electrons and holes. The value of the intrinsic concentration derived from statistical-mechanical arguments serves as a relationship among the kinetic parameters in equations (11) and (13).

The divergence of the current is zero at steady state; therefore the fluxes of holes and electrons are related by

$$\nabla \cdot \underline{N}_e - \nabla \cdot \underline{N}_h = 0 \quad . \tag{16}$$

A material balance on electrons, analogous to equation (8), could be used to replace equation (16).

Poisson's equation,

$$\nabla^2 \Phi = - \frac{F}{\epsilon_{sc}} [p - n + (N_d - N_a)] \quad , \tag{17}$$

relates the potential to the charge distribution. The Debye length,

$$\lambda_{sc} = \left(\epsilon_{sc} RT/F^2 (N_d - N_a) \right)^{1/2} \quad , \tag{18}$$

characterizes the distance over which the potential varies in the semiconductor. It typically has a value of 1×10^{-6} to 2×10^{-5} cm.

The degree of ionization of donors or acceptors is dependent upon the concentrations of charged species within the semiconductor and upon the temperature. Complete ionization is frequently assumed, and this assumption is reasonable at room temperatures.

2.2 Electrolyte

For dilute electrolytic solutions (less than 3 M) the flux of an ionic species can be separated into migrational, diffusional, and convective terms, i.e.,

$$\underline{N}_i = -z_i u_i c_i F \nabla \Phi - D_i \nabla c_i + c_i \underline{v} \ . \tag{19}$$

This relationship fails for concentrated solutions due to the neglect of the contributions of activity coefficients (see equation (3)) and to the neglect of ion-ion interactions.[N4] Under the assumption that homogeneous reactions do not take place, conservation of mass yields a uniform flux at steady-state, i.e.,

$$\nabla \cdot \underline{N}_i = 0 \ . \tag{20}$$

The potential and concentrations of charged species are related by Poisson's equation,

$$\nabla^2 \Phi = - \frac{F}{\epsilon_{sol}} \sum_i z_i c_i \ . \tag{21}$$

Electroneutrality of the electrolyte is not assumed here because the diffuse region near the interface plays an important role in the microscopic model of the interface. The Debye length in the solution is given by

$$\lambda_{sol} = \left(\frac{\epsilon_{sol} RT}{F^2 \sum_i z_i c_{i,\infty}} \right)^{1/2} , \tag{22}$$

and typically has a value of 1×10^{-8} to 1×10^{-7} cm.

The relationships presented above are sufficient to describe the electrolytic solution. An additional relationship yields the current density

as a function of the ionic fluxes,

$$i = F \sum_i z_i \underline{N}_i \ . \tag{23}$$

Within the semiconductor, this can be regarded to be an integrated form of equation (16).

2.3 Semiconductor-Electrolyte Interface

The interfacial reactions described in section 1.1 are driven by departure from equilibrium. For a general interfacial reaction,[N4]

$$\sum_i s_i M_i^{z_i} \rightarrow 0 \ , \tag{24}$$

the condition of equilibrium is given by

$$\sum_i s_i \mu_i = 0 \ . \tag{25}$$

Here, s_i is the stoichiometric coefficient of species i, M_i is a symbol for the chemical formula of species i, and μ_i is the electrochemical potential of species i. Electrons at a given energy level (or holes) are included explicitly as a reactant.

The rate of a reaction ℓ at the interface is given by

$$\begin{aligned} r_\ell = {} & k_{f,\ell} \exp\left(\frac{(1-\beta_\ell) nF\Delta\Phi_\ell}{RT} \right) \prod_i c_i^{p_{i,\ell}} \\ & - k_{b,\ell} \exp\left(\frac{-\beta_\ell \ nF\Delta\Phi_\ell}{RT} \right) \prod_i c_i^{q_{i,\ell}} \ , \end{aligned} \tag{26}$$

where β_ℓ is a symmetry factor (usually assumed to be equal to 1/2), $k_{f,\ell}$ and $k_{b,\ell}$ are forward and backward reaction rate constants, respectively, n is the number of electrons transferred, and $\Delta\Phi_\ell$ is the potential driving force for the given reaction, ℓ. The potential driving force enters into reactions involving charge transfer from locations of one potential to locations of another.

The reaction orders for a given species i in the forward and reverse directions are $p_{i,\ell}$ and $q_{i,\ell}$, respectively. They are determined from the stoichiometric coefficients, $s_{i,\ell}$:

$$\text{For } s_{i,\ell} = 0; \quad p_{i,\ell} = 0, \quad \text{and } q_{i,\ell} = 0.$$
$$\text{For } s_{i,\ell} > 0; \quad p_{i,\ell} = s_{i,\ell}, \quad \text{and } q_{i,\ell} = 0.$$
$$\text{For } s_{i,\ell} < 0; \quad p_{i,\ell} = 0, \quad \text{and } q_{i,\ell} = -s_{i,\ell}.$$

The reaction rates are written in terms of the equilibrium constants as

$$r_\ell = k_{b,\ell}\left\{ K_\ell \exp\left(\frac{(1-\beta_\ell)F\Delta\Phi_\ell}{RT} \right) \prod_i c_i^{p_{i,\ell}} - \exp\left(\frac{-\beta_\ell F\Delta\Phi_\ell}{RT} \right) \prod_i c_i^{q_{i,\ell}} \right\} . \tag{27}$$

The equilibrium constant used here is the ratio of the forward and backward rate constants:

$$K_\ell = \frac{k_{f,\ell}}{k_{b,\ell}} . \tag{28}$$

The equilibrium constants can be related to equilibrium interfacial concentrations and potentials, i.e.

$$K_\ell = \exp\left(- \frac{F}{RT} \Delta\Phi_\ell \right) \prod_i c_i^{-s_{i,\ell}} . \tag{29}$$

Through equation (27), the equilibrium constants can be related to electron-site and Fermi energies. Within parametric studies, it is convenient to allow one independent rate constant to be characteristic of each group of interfacial reactions. For example, adsorption reactions (IHP-OHP) might have individual rate constants for each reaction ℓ related to the characteristic rate constant by

$$k_{b,\ell} = k_j^{\circ} K_{\ell}^{-1/2} \quad , \tag{30a}$$

and

$$k_{f,\ell} = k_j^{\circ} K_{\ell}^{1/2} \quad , \tag{30b}$$

where k_j° is the pre-exponential part of the rate constant, with a characteristic value for a given reaction type j, and β was given a value of one half. The value for the equilibrium constant K_{ℓ} incorporates the energy levels of interfacial sites and associated energies of adsorption. These equations are consistent with equations (27) and (28).

The general approach described above can be applied to an arbitrarily complex interfacial reaction scheme. Material balances govern the interface. Under steady-state conditions, these are expressed by continuity of flux at the OSS and the OHP; i.e.,

$$\underline{N}_e \Big|_{oss} = \sum_{\ell} -s_{e,\ell} r_{\ell,oss} \quad , \tag{31a}$$

$$\underline{N}_h \Big|_{oss} = \sum_{\ell} -s_{h,\ell} r_{\ell,oss} \quad , \tag{31b}$$

and

$$\underline{N}_i \Big|_{ohp} = \sum_{\ell} -s_{i,\ell} r_{\ell,ohp} \quad . \tag{31c}$$

Material balances are also written for each adsorbed species i at the ISS and the IHP; i.e.,

$$\sum_{\ell} s_{i,\ell} \; r_{\ell,iss} = 0 \quad , \tag{32a}$$

and

$$\sum_{\ell} s_{i,\ell} \; r_{\ell,ihp} = 0 \quad . \tag{32b}$$

These equations apply only if surface states are involved within the

microscopic model of the interface.

Gauss's law can be applied to the region between the OSS and ISS:

$$\Phi_{oss} - \Phi_{iss} = \frac{\delta_1}{\epsilon_{sc}} \left(\frac{\epsilon_2}{\delta_2} (\Phi_{iss} - \Phi_{ihp}) + F\sum_{iss} z_i \Gamma_i \right) , \qquad (33a)$$

and between the ISS and the IHP:

$$\Phi_{iss} - \Phi_{ihp} = \frac{\delta_2}{\epsilon_2} \left(\frac{\epsilon_{sol}}{\delta_3} (\Phi_{ihp} - \Phi_{ohp}) + F\sum_{ihp} z_i \Gamma_i \right) , \qquad (33b)$$

where Γ_i are the surface concentrations of charges species located at the respective interfacial planes.

The approach described above allows description of interfacial reactions in terms of individual single-step processes. Frequently, reactions are described by a single rate expression. The rate of a charge-transfer reaction, for example, can be expressed through the Marcus-Gerischer theory by

$$r = k_{red} c_{red} \int_{-\infty}^{+\infty} \kappa(E) \rho(E) [1-f(E)] D_{red}(E) \, dE$$

$$- k_{ox} c_{ox} \int_{-\infty}^{+\infty} \kappa(E) \rho(E) f(E) D_{ox}(E) \, dE , \qquad (34)$$

where k_{ox} and k_{red} are rate constants, $\kappa(E)$ is an energy-dependent transmission or rate constant, $\rho(E)[1-f(E)]$ is the distribution of unoccupied electron states in the electrode, $\rho(E)f(E)$ is the distribution of occupied states in the electrode, and D_{ox} and D_{red} are the distributions of occupied and unoccupied states, respectively, for electrons associated with the ionic species.[G3-4,M13] This may be regarded to be a form of equation (26) integrated over all electron energy levels. Within this approach, the occupancy of electron states f(E) is given by the Fermi-Dirac distribution, and the energy states of electrons associated with ionic species are distributed according to

$$D_{red}(E) = \exp\left(- \frac{(E - E_{F,el} - \lambda)^2}{4kT\lambda} \right) , \tag{35a}$$

and

$$D_{ox}(E) = \exp\left(- \frac{(E - E_{F,el} + \lambda)^2}{4kT\lambda} \right) , \tag{35b}$$

where λ is called the rearrangement or reorientation energy. This term is used to relate the energy of electrons in the semiconductor to the energy of electrons associated with the ionic species. At equilibrium, the Fermi energy, or electrochemical potential, of electrons in the semiconductor is equal to the Fermi energy of electrons associated with the ionic species. This requirement specifies the concentrations of oxidized and reduced species at the semiconductor surface.

A kinetic argument can be used instead to establish the equilibrium distribution of ions at the semiconductor surface. The rate of adsorption of a species i is given according to equation (26) as

$$\begin{aligned} r_\ell = {} & k_{f,\ell} \exp\left(\frac{-z_i(1-\beta_\ell)F\Delta\Phi_\ell}{RT} \right) \Gamma_i \\ & - k_{b,\ell} \exp\left(\frac{z_i\beta_\ell \; F\Delta\Phi_\ell}{RT} \right) c_i(\Gamma_{ihp} - \sum_k \Gamma_k) \quad , \end{aligned} \tag{36}$$

Under equilibrium conditions the reaction rate is zero, and the fractional occupation of the inner Helmholtz plane is given by

$$\frac{\Gamma_i}{\Gamma_{ihp}} = \frac{c_i e^{-\Delta E_i/RT}}{1 + \sum_k c_k e^{-\Delta E_k/RT}} \tag{37}$$

where

$$\Delta E_i = -z_i F \Delta\Phi_\ell + RT \ln \left(\frac{k_{f,\ell}}{k_{b,\ell}} \right) . \tag{38}$$

The fractional occupation by a single species i corresponds to that given by the Langmuir adsorption isotherm (see, e.g., Delahay[D10]) for which ΔE_i is the "standard" free energy of adsorption. The "standard" free energy of adsorption is therefore a function of $\Delta\Phi_\ell$, the equilibrium potential difference between the inner and outer Helmholtz planes.

The equilibrium constants given in equation (29) couple the equilibrium concentrations of electrons, obtained as functions of Fermi energy, and the equilibrium concentrations of adsorbed ions, obtained as functions of concentration and free energies of adsorption.

2.4 Boundary Conditions

The boundary conditions are specified by the microscopic model of the various interfaces included within the photoelectrochemical cell. A metal-semiconductor interface, for example, can be described in a manner similar to that presented in the preceding section. Consider a semiconducting electrode bounded at one end by the electrolyte and at the other end by a metallic current collector. The boundary conditions at the semiconductor-electrolyte interface are incorporated into the model of the interface. Appropriate boundary conditions at the semiconductor-current collector interface are that the potential is zero, the potential derivative is equal to a constant, determined by the charge assumed to be located at the semiconductor-current collector interface, and all the current is carried by electrons (the flux of holes is zero). These conditions are consistent with a selective ohmic contact.[F5] The boundary conditions in the electrolytic solution are set a fixed distance from the interface. This distance may be considered to be a diffusion layer. The boundary conditions are that the potential gradient is continuous and that all concentrations have their bulk value.

2.5 Counterelectrode

In the region sufficiently far from the interface that electroneutrality holds and under the assumptions that the concentration is uniform and that the solution adjacent to the electrodes may be treated as equipotential surfaces, the potential distribution can be obtained through solution of Laplace's equation, $\nabla^2\Phi=0$, and is a function of current density. The potential drop in the region between the counterelectrode and the outer limit of the diffusion layer is given by

$$V_{IR} = \frac{Li}{\kappa} , \tag{39}$$

where κ is the solution conductivity and L is the distance between the counterelectrode and the outer edge of the diffusion layer. The counterelectrode was assumed here to be in a configuration parallel to the semiconductor. Relaxation of this assumption will be discussed in section 3.3 The conductivity of dilute solutions can be related to ionic mobilities and concentrations by

$$\kappa = F^2 \sum_i z_i^2 u_i c_i , \tag{40}$$

or is obtained from experimental measurements for a given electrolyte.

The potential drop across the counterelectrode-electrolyte interface is given by

$$V_{CE} = V_{CE}^{o} + \eta_{CE} , \tag{41}$$

where V_{CE}^{o} is the equilibrium potential drop across the interface and η_{CE} is the total counterelectrode reaction overpotential. The total overpotential is related to the current density through the Butler-Volmer reaction model[D10,N4]

$$i = i_o\left\{\left(1 - \frac{i}{i_{c,lim}}\right)\exp\left(\frac{(1-\beta)nF}{RT}\eta_{CE}\right) - \left(1 + \frac{i}{i_{a,lim}}\right)\exp\left(-\frac{\beta nF}{RT}\eta_{CE}\right)\right\} \tag{42}$$

where i_o is the exchange current density associated with the bulk concentrations of reactants, $i_{k,lim}$ is the diffusion-limited current density associated with species k, and n is the number of electrons transferred in the counterelectrode reaction.

3. Photoelectrochemical Cell Design

The liquid-junction photovoltaic cell has the advantages that the junction between electrolytic solution and semiconductor is formed easily and that polycrystalline semiconductors can be used. The principal disadvantage is that the semiconductor electrode tends to corrode under illumination. The electrochemical nature of the cell allows both production of electricity and generation of chemical products which can be separated, stored, and recombined to recover the stored energy. Liquid-junction cells also have the advantages that are attributed to other photovoltaic devices. Photovoltaic power plants can provide local generation of power on a small scale. The efficiency and cost of solar cells is independent of scale, and overall efficiency is improved by locating the power plant next to the load.[O1]

The design of a liquid-junction photovoltaic cell requires selection of an appropriate semiconductor-electrolyte combination and design of an efficent cell configuration. The selection of a semiconductor is based upon the band gap, which provides an upper limit to the conversion efficiency of the device, and the choice of electrolyte is governed by the need to limit corrosion and by the requirement that interfacial reaction rates be fast.

3.1 Choice of Materials

The performance of photoelectrochemical cells constructed with thin-film or polycrystalline semiconductors is strongly dependent upon the method of film formation and upon the surface preparation. Conversion efficiencies (incident solar illumination to electrical power) of 3 to 6.5 percent have been reported for cells using thin-film n-CdSe electrodes (see references R12, K8, L13-14, P9, R3, R8-9, and H14), and a conversion efficiency of 5.1 percent has been achieved with a pressure-sintered polycrystalline CdSe photoelectrode.[M16] A comparable efficiency of 8.1 percent has been reported for a single-crystal CdSe electrode.[H6] Conversion efficiencies of 0.038 to 0.3 percent have been reported for polycrystalline CdS films[M15,P8,T4] as

compared to 1.3 percent for single-crystal CdS.[H6] Conversion efficiencies of up to 7.3 percent have been reported for polycrystalline n-GaAs films;[H7,J2,N6] 12 percent has been reported for the single crystal n-GaAs.[H8,P4] The lower efficiency of the polycrystalline thin-film semiconductors, as compared to the single-crystal counterparts, is expected to be compensated by their lower cost. Reviews of the materials aspects of photoelectrochemical cells are given in references C1, C10, and M23.

3.1.1 **Band gap.** An upper limit to the efficiency of photovoltaic devices can be established, based upon the band gap and the solar spectrum, without consideration of cell configuration. This ultimate efficiency is given by[A8]

$$\eta_{ult} = \frac{E_g \int_{E_g}^{\infty} N(E)\, dE}{\int_{0}^{\infty} E\, N(E)\, dE} \tag{43}$$

where E_g is the semiconductor band-gap energy, E is the photon energy, and N(E) is the number density of incident photons with energy E. The fraction of the power in the solar spectrum that can be converted to electrical power is a function of the band gap of the semiconductor. Photons with energy less than the band gap cannot produce electron-hole pairs. Photons with energy greater than the band gap yield only the band gap energy.[L15-16,W15]

The ultimate efficiency of equation (43) represents an upper limit to conversion of solar energy;[A8,W12,S3] factors such as reflection and absorption losses of sunlight, kinetic and mass transfer limitations, and recombination will reduce the efficiency. These effects are included in section 3.3. A band gap between 1.0 and 1.5 eV is generally considered to be appropriate for efficient conversion of solar energy.

3.1.2 **Corrosion.** The application of liquid-junction technology to photovoltaic power conversion is limited by problems associated with the semiconductor-electrolyte interface. Primary among these problems is corrosion. Efficient conversion of solar energy requires a band gap between 1.0 and 1.5 eV, and most semiconductors near this band gap corrode readily under illumination. Semiconductors with large band-gaps (4 to 5 eV) tend to

be more stable but cannot convert most of the solar spectrum.

Among the approaches taken to solve this problem, the most successful concern the matching of an electolyte to the semiconductor. The rate of corrosion is reduced if the semiconductor is in equilibrium with the corrosion products. The rate of corrosion can also be reduced by using a redox couple which oxidizes easily. The oxidation of the redox couple Se_{x+1}^{2-}/Se_x^{2-} for example, has been shown to compete successfully with photocorrosion reactions for holes in n-type GaAs electrodes.[H10,C4]

P-type semiconductors used as cathodes are more stable than the more common and generally more efficient n-type semiconducting anodes. The inefficiency of p-type photocathodes has been attributed to the presence of surface states near the valence band energy. A stable p-type photocathode has been developed, however, with a solar-energy-conversion efficiency of 11.5 percent.[H9] Protective films have been proposed to be a solution to electrode corrosion. The electrode, in this case, would be a small band-gap semiconductor covered by a film composed of either a more stable large band-gap semiconductor, a conductive polymer, or a metal. A large Schottky barrier is freqently present at such semiconductor-metal and semiconductor-semiconductor interfaces which blocks the transfer of holes from the semiconductor to the electrolyte. In cases where the photocurrent is not blocked, corrosion can take place between the semiconductor and the protective film.[M12,G7] Menezes et al.[M14] discuss the difficulties in avoiding absorptive losses in the metal film while maintaining sufficient integrity to serve the semiconductor corrosion protection function. Frese et al.[F8] have, however, reported a measurable improvement in the stability of GaAs with less than a monolayer gold metal coverage. Thin conductive poly-pyrrole films appear to be successful in inhibiting corrosion in some electrolytes.[N7-8,S9-10,F3,B10,R5] In addition, insulating polymer films deposited on grain boundaries can improve the performance of polycrystalline semiconductors by reducing surface recombination rates.[W3] (For more complete reviews of the corrosion of semiconducting electrodes, see references W14, H10, H4, M12, M21, K9, and G6-7).

3.2 Solution of the Governing Equations

Quantitative optimization or prediction of the performance of photoelectrochemical cell configurations requires solution of the macroscopic transport equations for the bulk phases coupled with the equations associated with the microscopic models of the interfacial regions. Coupled phenomena govern the system, and the equations describing their interaction cannot, in general, be solved analytically. Two approaches have been taken in developing a mathematical model of the liquid-junction photovoltaic cell: approximate analytic solution of the governing equations and numerical solution.

3.2.1. Analytic approach. The semiconductor electrode is typically divided into three regions. Surface-charge and electron and hole-flux boundary conditions model the semiconductor-electrolyte interface. The region adjacent to the interface is assumed to be a depletion layer, in which electron and hole concentrations are negligible. The potential variation is therefore independent of hole and electron concentration in this region. Far from the interface a neutral region is defined in which the potential is constant; here electron and hole fluxes are driven only by diffusion. Current-potential relationships are derived in the analytic approach by invoking assumptions appropriate to each region.

Integration of Poisson's equation in the depletion layer, for example, results in a depletion layer thickness W in terms of the voltage drop V across the layer:

$$W = \left(\frac{2\epsilon V}{F(N_d - N_a)} \right)^{\frac{1}{2}} . \qquad (44)$$

The depletion layer thickness is, as shown in Figure 3, a function of illumination intensity. The assumption that the semiconductor can be separated into depletion and neutral regions restricts the voltage drop V to values high enough to deplete the majority carriers (electrons in an n-type semiconductor) in a region adjacent to the interface but small enough to avoid formation of an inversion layer (in which the concentration of minority carriers is significant). This assumption is not appropriate under many operating conditions for which the liquid-junction cell may be practical. (Figure 4, for example, shows an inversion layer adjacent to the solution interface.)

Analytic models of photoelectrochemical devices closely resemble models of solid-state solar cells (see, e.g., references A7, C5-6, D9, K11, M17, P1, S5, S12,, S14, T1-2, and V1). Several analytic current-voltage relationships have been derived which use the general approach described above and differ in their treatment of surface reactions and recombination within the depletion and neutral layers. Gartner[G2] neglected recombination and thermal generation of carriers in the depletion region and neglected the effect of concentration limitations at the semiconductor-electrolyte interface. The Gartner model is frequently used to analyze experimental results.[B12,K6,W7] Wilson[W8-9] used the same approach but included surface recombinations. Albery et al.[A4-6] extended the model of Gartner by including recombination of holes and electrons in the depletion layer. Reichman[R6-7] presented a model which included recombination in the depletion region and kinetic limitation at the interface. Reiss[R10] presented models for various cases, including within the model the potential drop across the electrolyte double layer, surface recombination, and surface kinetic limitations. The semiconductor was divided into depletion and neutral regions, and the effect of illumination on cell potential was included as an additive photovoltage. Ahlgren[A2] incorporated a Butler-Volmer reaction rate expression into the boundary conditions at the semiconductor-electrolyte interface. McCann and Haneman[M8] included enhanced recombination associated with grain boundaries within the bulk of the semiconductor. The photovoltage was included in the calculation of the depletion region width. McCann et al.[M9] used an analytic model to calculate the current-voltage characteristics of front and back-wall-illuminated liquid-junction cells.

Surface states and crystal imperfections have been found to play an important role in charge-transfer and redox reactions at the semiconductor-electrolyte interface (see references H12, W6, W11, A3, A9, B3, F2, B6, and N1). Mathematical and conceptual relationships have been developed which describe electrochemical reactions at the semiconductor-electrolyte interface in terms of surface states and potentials (see, e.g., references G1, J1, M4, G4, M20, B7, M11, M13, F7, K7, and R4). Electrochemical reaction via surface states has been included within an analytic model,[C7] but this model is still limited by the restrictions described above.

Equivalent circuit models of the liquid-junction cell have also been presented.[S6,M6-7] These models are useful in the analysis of impedance response measurements.

3.2.2. **Numerical approach.** Use of a digitial computer in the numerical solution of the equations governing the liquid-junction cell eliminates the need for restrictive assumptions. This approach has been used in the modeling of solid-stage devices.[M1,D6-7,C8-9,S16,H2,L1-2,R1] Laser and Bard[L7-10] developed a computer program which was used to calculate open-circuit photopotentials, the transient behavior of the system following charged injection, and the time dependence of photocurrents in liquid-junction cells. Time dependent material balances of holes and electrons and Poisson's equation described the semiconductor. The interface was included in terms of charge and flux boundary conditions. The model was limited by lack of convergence for electrode thicknesses greater than that of the space-charge region and did not treat explicitly the electrolyte and counterelectrode. Orazem and Newman[O5-7] present a numerical solution of the governing equations that includes analysis of neutral, space-charge, and inversion regions in the semiconductor coupled with explicit treatment of the electrolyte and the counterelectrode. Interfacial reactions were treated explicity. Potential-dependent concentration variables were defined to reduce the numerical difficulties associated with concentrations that can vary up to 20 orders of magnitude in a short distance.[O5,B8] Errors associated with matching of solutions for various regions of the semiconductor were thereby avoided. Numerical methods for solving coupled ordinary differential equations are discussed by Newman and associates,[N3,W5] and a general method for treating boundary conditions is presented by White.[W4]

A number of computer programs related to the liquid-junction photovoltaic cell have been developed. Leary et al.,[L11] for example, calculated carrier concentrations in polycrystalline films using a numerical solution of Poisson's equation coupled with overall charge neutrality within spherical grains. Their model was used for analysis of semiconductor gas sensors. Davis and colleagues[D3-5] presented a computer program which uses simultaneous calculation of surface and solution equilibrium states to obtain the equilibrium condition of electrical double layers.

3.3 The Influence of Cell Design

The optimal design of liquid-junction photovoltaic cells shares constraints with solid-state photovoltaic cells.[H15,I1] Current collectors cast shadows and can reduce the amount of sunlight absorbed in the semiconductor. A constraint unique to the liquid-junction cell is the placement of the counterelectrode relative to the semiconductor-electrolyte interface. Shadows, which reduce efficiency and cause local currents in solid-state photovoltaic cells, may lead to localized corrosion in photoelectrochemical cells. Mass-transfer and kinetic limitations at the counterelectrode and resistance of the electrolyte can play important roles in the optimal design of the liquid-junction photovoltaic cell. These considerations are treated qualitatively by Parkinson.[P5]

Ideally, modeling and optimization of photoelectrochemical cell configurations involves solution of the governing equations in three dimensions. A first approach toward the analysis of these devices involves coupling the solution of the one-dimensional equations (see the previous section) with primary resistance calculations for the specific cell configuration. The computational problem is still difficult but can be solved. This approach toward calculation of the influence of cell design is illustrated below and is based on the work of Orazem and Newman.[O8] The system modeled was an n-type GaAs semiconducting anode in contact with an 0.8 M K_2Se, 0.1 M K_2Se_2, 1.0 M KOH electrolytic solution. The choice of this semiconducting electrode system was based upon the work of Heller and associates.[H10] The semiconductor was assumed to be in the form of a thin film (see Mitchell for a review of thin-film photovoltaic technologies[M18]). Interfacial reactions were included but were not limited by kinetics.[O5-7] This approach requires calculation of the resistance to current flow associated with the two-dimensional systems. Some methods for calculation of this resistance were reviewed by Fleck et al.[F4] Kasper,[K1-5] Moulton,[M22] Newman,[N5] and Orazem and Newman[O4] have presented primary resistance calculations for configurations of potential application to photoelectrochemical cells.

One possible photoelectrochemical cell configuration employs a slotted-semiconductor electrode as presented in Figure 7a. A glass cover plate protects the cell. Sunlight passes through the cover plate and the electrolyte to illuminate the semiconductor surface. Electrical current passes between the semiconductor and the counterelectrode through slots cut in the semiconductor. Characteristic features of this configuration are that no shadows are cast upon the semiconductor and that reaction products could be separated if a membrane were placed between the semiconductor and the counterelectrode.

A two-dimensional representation of this cell is presented in Figure 7b. The primary current distribution and the resistance of a cell containing a slotted electrode were calculated using numerical methods coupled with the Schwarz-Christoffel transformation.[O4,B9,A1] The cell resistance is a function of three geometric ratios, chosen to be t/G, h/G, and L/h, where L is the half-length of the protruding electrode assembly, t is the thickness of the protruding electrode assembly, G is the half-gap between the electrode assemblies, and h is the separation between the electrode and the upper insulating wall. The separation between the counterelectrode and the lower edge of the semiconductor-electrode assembly is also given by h. These parameters are shown in Figure 7c.

Four geometric parameters characterize this cell design. The distance between the counterelectrode and the semiconductor assembly was chosen to be 0.5 cm, and the semiconductor assembly thickness was assumed to be 0.1 cm. The values chosen for this analysis were based on mechanical considerations. Smaller spacing could result in shorting of counterelectrode and semiconductor and/or trapping of gas bubbles. The influence of the counterelectrode could be reduced by increasing the flow rate or degree of mixing near the counterelectrode, thereby increasing the limiting current. Interfacial reactions were considered to be equilibrated. Kinetic limitations at the semiconductor-electrolyte interface may greatly reduce the performance of some semiconductor systems.

The primary resistance for this system is presented in Figure 8 as a function of L/D with h/G as a parameter. The maximum power density is presented in Figure 9 as a function of L/h with h/G as a parameter. The maximum power density for this system is obtained with a small gap. For

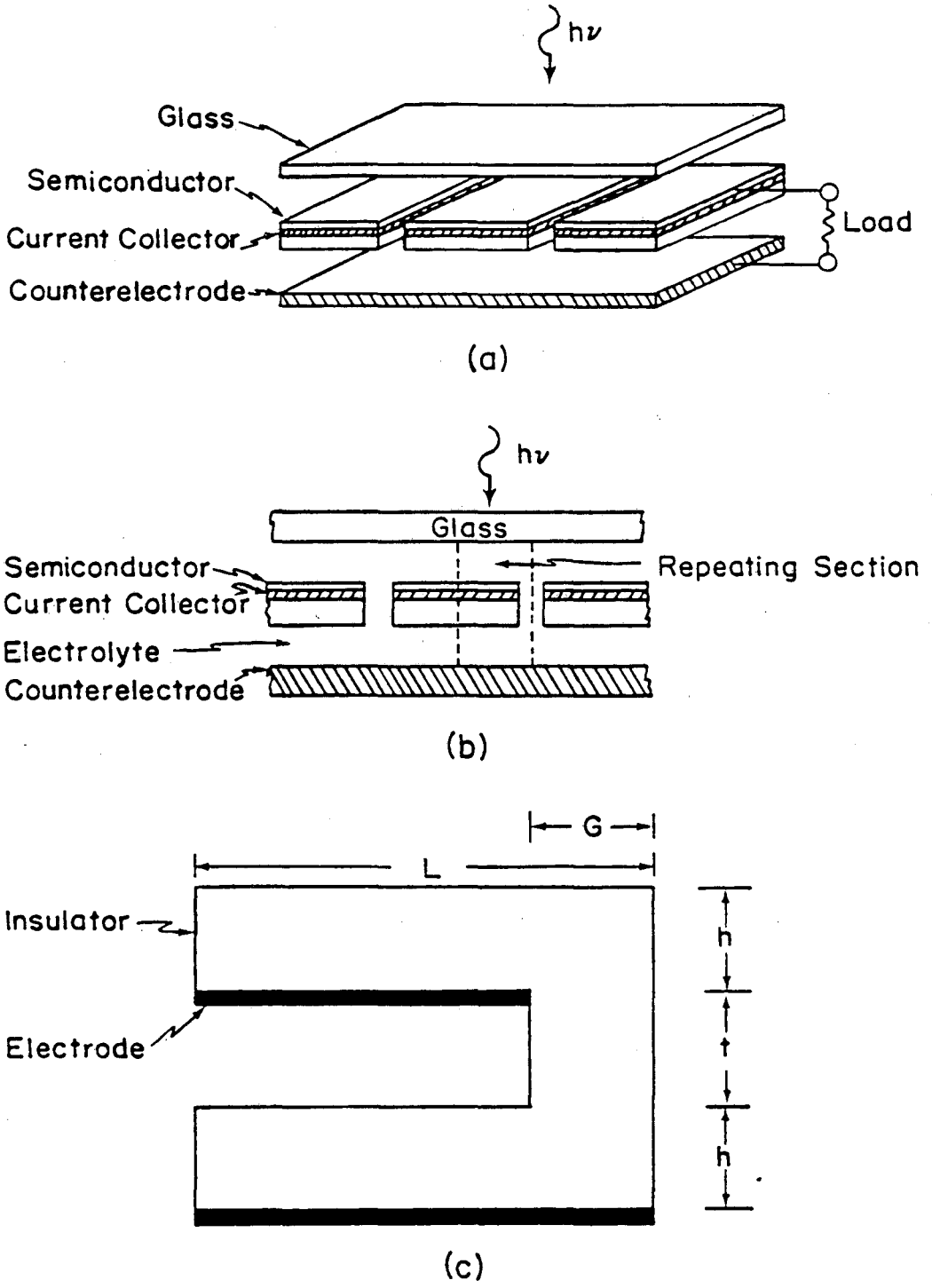

Figure 7. Slotted-electrode photoelectrochemical cell; (a) three-dimensional configuration, (b) two-dimensional representation, and (c) repeating section.

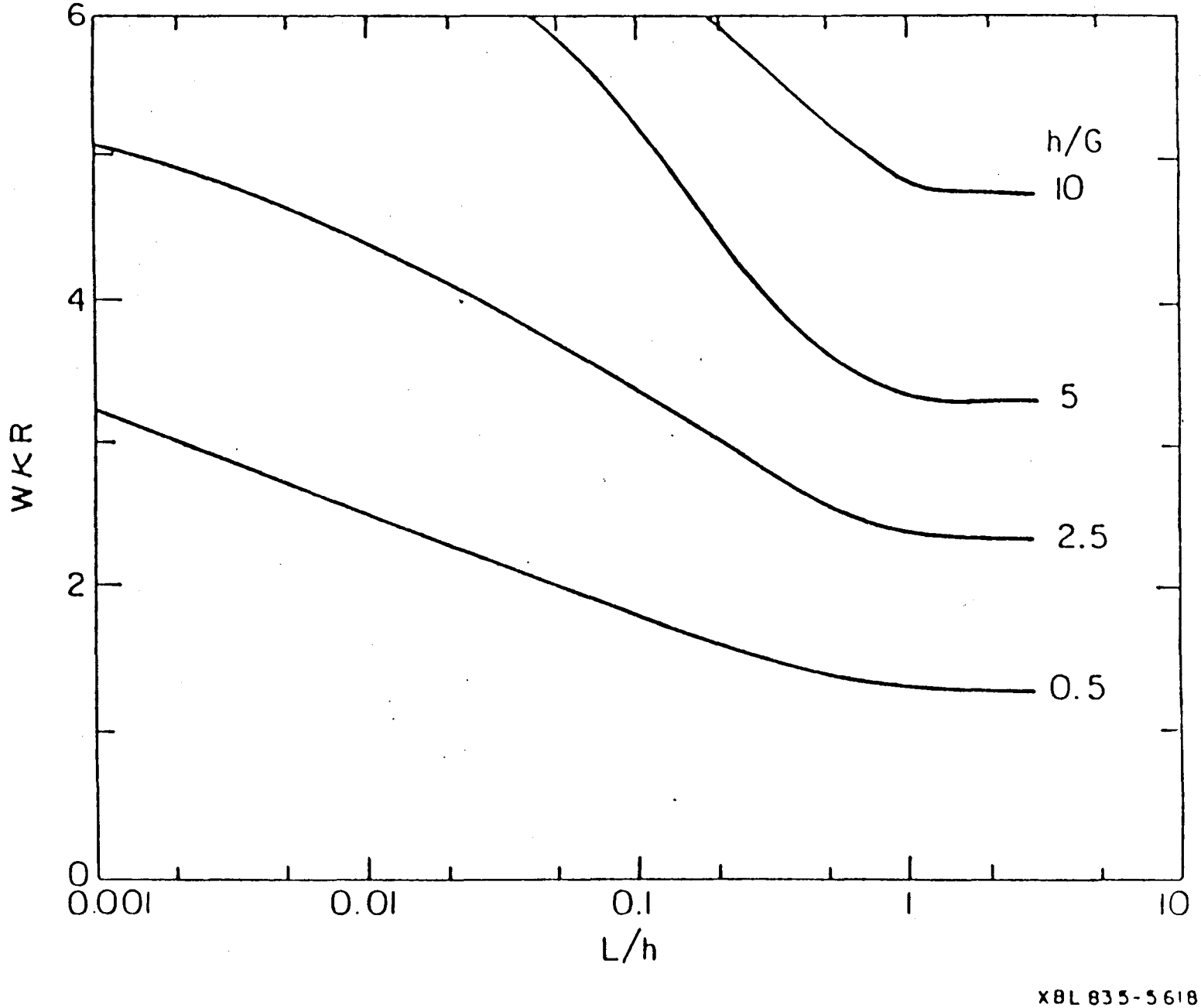

Figure 8. Primary resistance of a slotted-electrode cell as a function of L/h.

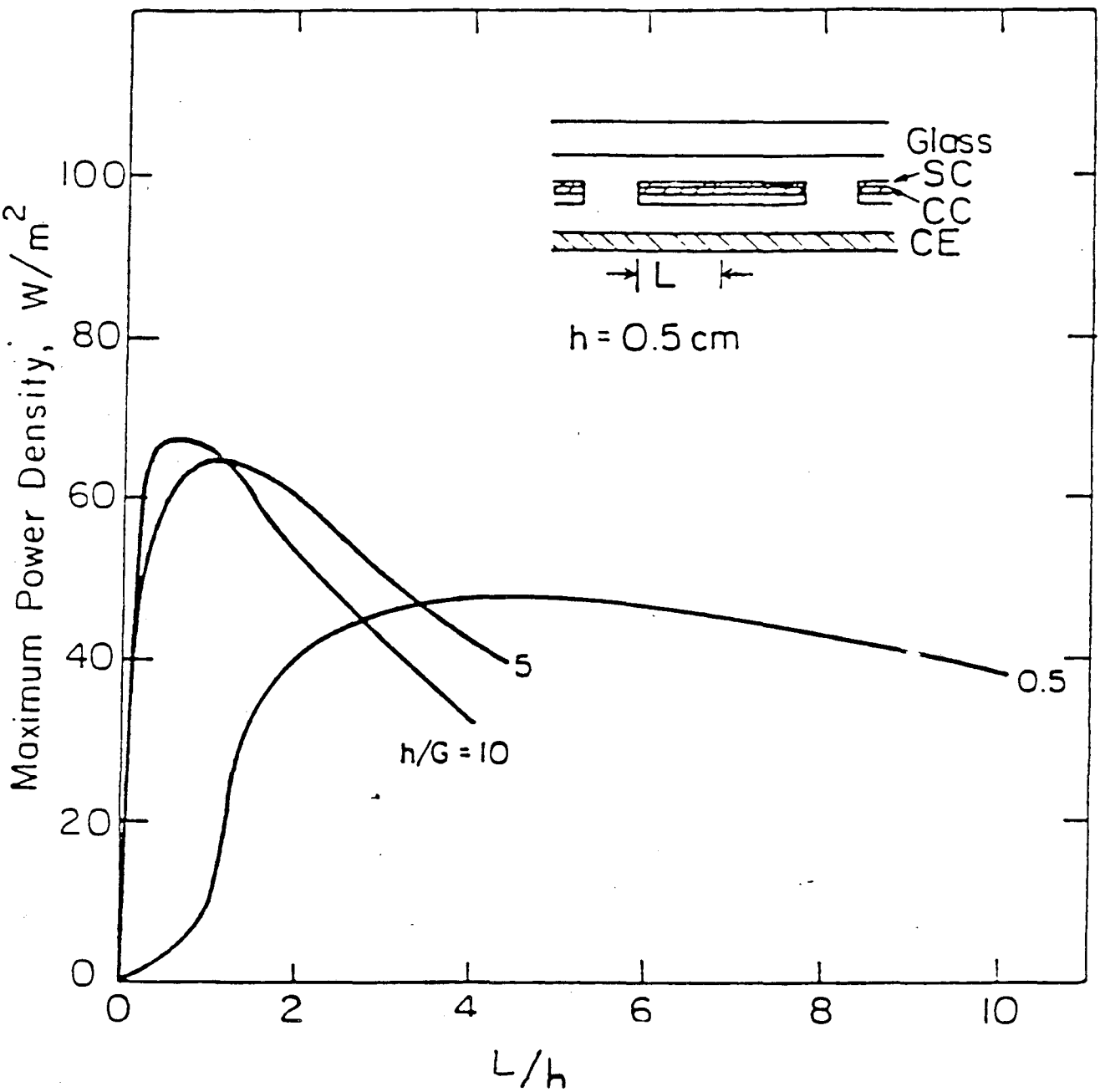

XBL 831-7975 A

Figure 9. Maximum power density as a function of L/h for the slotted-electrode photoelectrochemical cell.

h/G=0.5 (G=1 cm), the maximum power density was 47.8 W/m^2, and the maximum power efficiency was 5.4 percent. The current density under maximum power conditions was 15 mA/cm^2 delivered at 477.6 mV. For h/G=10 (G=0.05 cm), the maximum power density was 67.7 W/m^2, and the maximum power efficiency was 7.7 percent. At maximum power the current density was 15.2 mA/cm^2 delivered at 534.6 mV.

The hierarchy of photovoltaic cell efficiencies is presented in Table 1. Semiconductor effects, such as recombination, reduce the power efficiency of a GaAs-based device from a value of 37 percent, based solely upon band gap, to 15.3 percent. Reflection losses, with an arbitrarily chosen 80 percent efficiency of illumination, reduce this value to 12.2 percent. This value is consistent with the value measured in a bench-top experimental system for which the influence of counterelectrode limitations and electrolyte resistance can be minimized. This value can also be compared to the 12 percent efficiency obtained in the experimental work of Heller and Miller.[H8,H10,P4] Accounting for the effect of cell design reduces the efficiency from 15.3 percent to 9.8 percent, and inclusion of illumination losses further reduces the cell efficiency to 7.7 percent for the slotted-electrode cell.

Table 1. Power Efficiency under Front Illumination

	No Illumination Losses	Illumination Losses*	Experimental Results[H8,H10,P4]
Optimal Band-Gap	45	36 (80%)	
GaAs Band-Gap	37	30 (80%)	
Semiconductor-Electrolyte Junction	15.3	12.2 (80%)	12.0
Slotted-Electrode Cell Design	9.8	7.7 (55.4%)	

* In some cases, the number in parenthesis represents the fraction of AM-2 illumination (above the bandgap) which actually enters the semiconductor, after accounting for reflection, shadowing, and absorption in intervening phases. In other cases, where detailed calculations were not made, it represents the ratio to column 1 because the nonlinear effect of illumination could not be assessed.

The maximum power efficiency is presented as a function of illumination intensity in Figure 10 for the slotted-electrode cell. The cell was designed with the design parameters calculated to be optimal under peak AM-2 illumination. The power efficiency decreases with increasing illumination due to the influence of electrolyte resistance and kinetic and mass-transfer limitations at the counterelectrode. These phenomena become increasingly important as current densities increase, and mass-transfer limitations at the counterelectrode can result in an upper limit for cell currents.

The maximum power efficiency for the system without counterelectrode limitations is also presented in Figure 10. These results are consistent with the use of a porous counterelectrode in the cell. The maximum cell current obtained under large magnitudes of illumination depends upon the ratio of the counterelectrode area to the semiconductor area. This ratio must be large for liquid-junction photovoltaic cells designed for large intensities of illumination, and for some configurations, a porous counterelectrode may be appropriate.[C2] Inclusion of a cooling system in the cell design becomes important under these conditions. The electrolyte itself can serve as a heat exchange medium in photoelectrochemical systems.

Similar calculations were performed for a cell with a wire-grid counterelectrode through which sunlight passes.[O8] Current-potential curves are presented in Figure 11 for these optimally designed cells as compared to the cell without interfacial kinetic limitations, counterelectrode limitations, or electrolytic resistance. The cell with a slotted semiconductor has a larger power efficiency than the wire-grid counterelectrode cell and can be designed for separation of chemical products. The analysis of the system designed for separation of chemical products would need to include the electrical resistance of the membrane.

The allowable capital investment for a photovoltaic cell is given by

$$I = 8.76\ P_{in}\ \eta\ \Delta c\ y_e, \tag{45}$$

where P_{in} is the annual incident illumination intensity averaged over 24 hours in W/m^2 (on this basis, the average insolation of the continental United States is 200 to 250 W/m^2.[A8]), η is the cell efficiency, Δc is the difference in selling price and operating cost in \$/kW-hr, and y_e is the break-even point

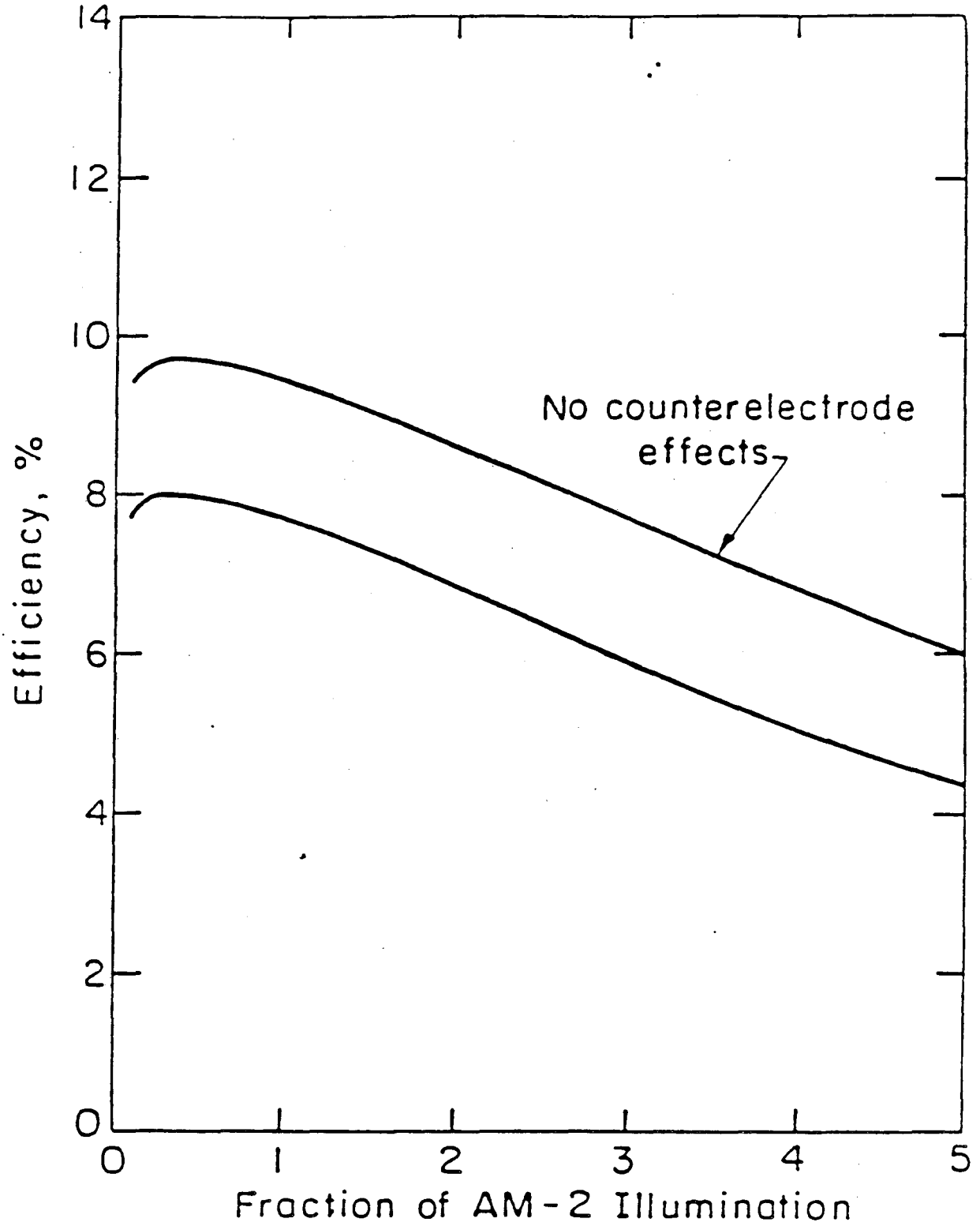

XBL 835-5616

Figure 10. Maximum power efficiency as a function of the fraction of peak AM-2 illumination for a slotted-electrode photoelectrochemical cell with h/G=10 and L/h=0.5.

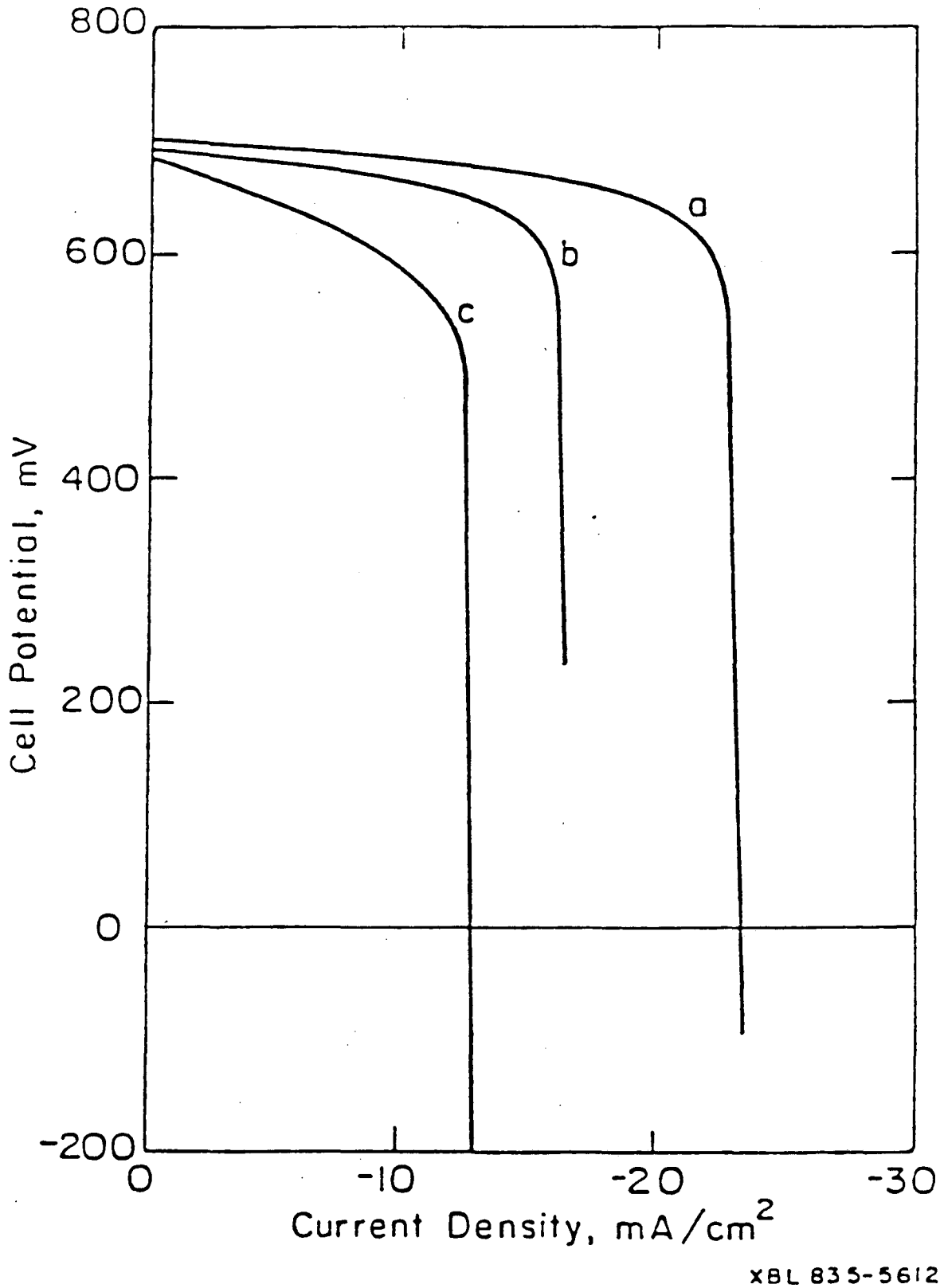

Figure 11. Cell potential as a function of current density for (a) a front-illuminated semiconductor without kinetic, electrolyte resistance, and counterelectrode limitations; (b) an optimally designed slotted-electrode cell with a porous counterelectrode; and (c) an optimally designed cell with a wire-grid counterelectrode of radius 0.5 cm.

in years. Lenses or mirrors could be used to increase the amount of sunlight striking the semiconductor surface. Based upon a 7.7 percent power efficiency (averaged over 24 hours), 250 W/m^2 incident illumination (averaged over 24 hours), \$0.05/kW-hr profit, and a break-even period of 5 years, an investment of $\$42/m^2$ is justified for the complete cell. Based upon a 15.3 percent power efficiency (this number is averaged over 24 hours and neglects the influence of cell design), an investment of $\$83/m^2$ is justified for the complete cell.

An increase of solar illumination by a factor of five while reducing the efficiency to 6 percent (see Figure 10) yields an acceptable initial investment of $\$164/m^2$. If the mirrors and lenses needed to concentrate sunlight are cheaper than the semiconducting film, the cell may be most economical under high illumination. The values presented here can be compared to the cost estimate of \$0.34 per peak watt presented by Weaver et al.[W2] for a GaAs photoelectrochemical cell. Their estimate is based on materials cost and assumes a cell efficiency of 13 percent. The influence of cell design was therefore neglected. Under AM-2 illumination, this value corresponds to $\$39/m^2$.

4. Conclusions

Development of a mathematical model of photoelectrochemical devices requires treatment of the diffuse double layer (or space charge region) in the semiconductor. The principles of electrochemical engineering can be readily applied to provide a chemical description of these devices in terms of potentials and concentrations of charged species. The macroscopic transport relations which govern the electrolyte and the semiconductor are coupled by a microscopic model of the interface. Analytic solution of the governing equations requires restrictive assumptions. These assumptions can be avoided by numerical solution of the governing equations.

The optimization of photoelectrochemical devices for solar energy conversion depends on the choice of semiconductor, electrolyte, and cell design. The performance of the cell is strongly dependent upon the design, surface area, and placement of the counterelectrode and current collectors. This type of solar cell may be economical under concentrated illumination or in regions where electrical power has high value.

5. Notation

5.1 Roman Characters

c_i	molar concentration of species i, mol/cm^3
D_i	diffusivity of species i, cm^2/s
E_i	energy of species or site i, eV
ΔE_i	ionic adsorption energy, J/mol
f_i	molar activity coefficient of species i
F	Faraday's constant, 96,487 C/equiv
G_{th}	rate of thermal electron-hole pair generation, $mol/s\text{-}cm^3$
G_L	rate of photo electron-hole pair generation, $mol/s\text{-}cm^3$
i	current density, mA/cm^2
i_o	exchange current density, mA/cm^2
$k_{f,\ell}$	forward reaction rate constant for reaction ℓ
$k_{b,\ell}$	backward reaction rate constant for reaction ℓ
k_k	rate constants for homogeneous reaction k
K_ℓ	equilibrium constant for reaction ℓ
m	solar absorption coefficient, 1/cm
M_i	symbol for chemical formula of species i
n	number of electrons involved in electrode reaction
n	electron concentration, mol/cm^3
n_i	intrinsic electron concentration, mol/cm^3
N	total site concentration, mol/cm^3
N_a	total bulk electron-acceptor concentration, mol/cm^3
N_d	total bulk electron-donor concentration, mol/cm^3
N_i	flux of species i, mol/cm^2s
p	hole concentration, mol/cm^3

$p_{i,\ell}$ heterogeneous reaction order

$q_{i,\ell}$ heterogeneous reaction order

q_o incident solar flux, mol/s-cm^2

r_ℓ heterogeneous reaction rate, mol/s-cm^2

R universal gas constant, 8.3143 J/mol-K

R_i net rate of production of species i, mol/s-cm^3

R_{rec} net rate of electron-hole recombination, mol/s-cm^3

s_i stoichiometric coefficient of species i in an electrode reaction

T absolute temperature, K

u_i mobility of species i, cm^2-mol/J-s

V potential drop across depletion layer, V

W depletion layer thickness, cm

z_i charge number of species i

5.2 Greek Characters

β symmetry factor

Γ_k surface concentration of energy or species k, mol/cm^2

δ_k distance between interfacial planes (gap denoted by k), cm

ϵ permittivity, C/V-cm

η photon efficiency

η_k total overpotential at interface k, V

θ fractional occupation of surface sites

κ conductivity, mho/cm

λ Debye length, cm

μ_i electrochemical potential of species i, J/mol

ϕ electrical potential, V

5.3 Superscripts

o	equilibrium
θ	secondary reference state at infinite dilution
*	secondary reference state in semiconductor

5.4 Subscripts

bulk	associated with the bulk
c	associated with conduction band in semiconductor
CE	associated with the counterelectrode
cell	associated with the cell
e	relating to electrons
h	relating to holes
ihp	associated with inner Helmholtz plane
iss	associated with inner surface states
ℓ	associated with reaction ℓ
o	equilibrium value or initial value
ohp	associated with outer Helmholtz plane
oss	associated with outer surface states
sc	associated with semiconductor
sol	associated with solution
v	associated with valence band in semiconductor

6. References

A1 Abramowitz, Milton, and Irene A. Stegun, Handbook of Mathematical Functions, Dover Publications, Inc., New York, 1964.

A2 Ahlgren, William L., "Analysis of the Current-Voltage Characteristics of Photoelectrolysis Cells," Journal of the Electrochemical Society, 128 (1981), 2123-2128.

A3 Ahmed, Syed M., and H. Gerischer, "Influence of Crystal Surface Orientation on Redox Reactions at Semiconducting MoS_2," Electrochimica Acta, 24 (1979), 705-711.

A4 Albery, W. John, Phillip N. Bartlett, Andrew Hamnett, and Martin P. Dare-Edwards, "The Transport and Kinetics of Minority Carriers in Illuminated Semiconductor Electrodes," Journal of the Electrochemical Society, 128 (1981), 1492-1501.

A5 Albery, W. John, and Phillip N. Bartlett, "The Recombination of Photogenerated Minority Carriers in the Depletion Layer of Semiconductor Electrodes," Journal of the Electrochemical Society, 130 (1983), 1699-1706.

A6 Albery, W. John, and Phillip N. Bartlett, "The Transport and Kinetics of Photogenerated Carriers in Colloidal Semiconductor Electrode Particles," Journal of the Electrochemical Society, 131 (1984), 315-325.

A7 Araujo, G. L., and E. Sanchez, "Analytical Expressions for the Determination of the Maximum Power Point and the Fill Factor of a Solar Cell," Solar Cells, 5 (1982), 377-386.

A8 Archer, M.D., "Electrochemical Aspects of Solar Energy Conversion," Journal of Applied Electrochemistry, 5 (1975), 17-38.

A9 Aruchamy, A., and Mark S. Wrighton, "A Comparison of the Interface Energetics for n-Type Cadmium Sulfide- and Cadmium Telluride-Nonaqueous Electrolyte Junctions," Journal of Physical Chemistry, 84 (1980), 2848-2854.

A10 Aymerich-Humet, X., F. Serra-Mestres, and J. Millan, "An Analytical Approximation for the Fermi-Dirac Integral $F_{1/2}(\eta)$," Solid State Electronics, 24 (1981), 981-982.

B1 Bard, Allen J., "Photoelectrochemistry and Heterogeneous Photocatalysis at Semiconductors," Journal of Photochemistry, 10 (1979), 59-75.

B2 Bard, Allen J., "Photoelectrochemistry," Science, 207 (1980), 139-144.

B3 Bard, Allen J., Andrew B. Bocarsly, Fu-Ren F. Fan, Erick G. Walton, and Mark S. Wrighton, "The Concept of Fermi Level Pinning at Semiconductor-Liquid Junctions. Consequences for Energy Conversion Efficiency and Selection of Useful Solution Redox Couples in Solar Devices," Journal of the American Chemical Society, 102 (1980), 3671-3677.

B4 Belloni, Jacqueline, Genevieve Van Amerongen, Michel Herlem, Jean-Lou Sculfort, and Rudolf Heindl, "Photocurrents from Semiconductor-Liquid Ammonia Junctions," Journal of Physical Chemistry, 84 (1980), 1269-1270.

B5 Bird, R Byron, Warren E. Stewart, and Edwin N. Lightfoot, Transport Phenomena, John Wiley and Sons, New York, 1960.

B6 Bocarsly, Andrew B., Dana C. Bookbinder, Raymond N. Dominey, Nathan S. Lewis, and Mark S. Wrighton, "Photoreduction at Illuminated p-Type Semiconducting Silicon Photoelectrodes. Evidence for Fermi Level Pinning," Journal of the American Chemical Society, 102 (1980), 3683-3688.

B7 Bockris, J. O'M., and K. Uosaki, "The Theory of the Light-Induced Evolution of Hydrogen at Semiconductor Electrodes," Journal of the Electrochemical Society, 125 (1978), 223-227.

B8 Bogatov, N. M., L. I. Gromovoi, M. B. Zaks, and E. V. Lelyukh, "A Numerical Solution of the One-Dimensional Boundary Value Problem of Charge Transfer in Solar Cells," Geliotekhnika, 18 (1982), 7-14.

B9 Bowman, F., Introduction to Elliptic Functions with Applications, John Wiley and Sons, Inc., New York, 1953.

B10 Bull, Randy A., Fu-Ren F. Fan, Allen J. Bard, "Polymer Films on Electrodes VII. Electrochemical Behavior at Polypyrrole-Coated Platinum and Tantalum Electrodes," Journal of the Electrochemical Society, 129 (1982), 1009-1015.

B11 Butler, M. A., R. D. Nasby, and Rod K. Quinn, "Tungsten Trioxide as an electrode for Photoelectrolysis of Water," Solid State Communications, 19 (1976), 1011-1014.

B12 Butler, M. A., "Photoelectrolysis and Physical Properties of the Semiconducting Electrode WO_3," Journal of Applied Physics, 48 (1977), 1914-1920.

C1 Cahen, David, Joost Manassen, and Gary Hodes, "Materials Aspect of Photo-Electrochemical Systems," Solar Energy Materials, 1 (1979), 343-355.

C2 Canfield, Duane, and S. Roy Morrison, "Electrochemical Storage Cell Based on Polycrystalline Silicon," Lawrence Berkeley Laboratory Report, LBL-14639, 1982.

C3 Card, D. C., and H. C. Card, "Interfacial Oxide Layer Mechanisms in the Generation of Electricity and Hydrogen by Solar Photoelectrochemical Cells," Solar Energy, 28 (1982), 451-460.

C4 Chang, K. C., A. Heller, B. Schwartz, S. Menezes, and B. Miller, "Stable Semiconductor Liquid-Junction Cell with 9% Solar to Electrical Conversion Efficiency," Science, 196 (1977), 1097-1098.

C5 Charles, J. P., M. Zaghdoudi, P. Mialhe, and A. Marrakchi, "An Analytical Model for Solar Cells," Solar Cells, 3 (1981), 45-56.

C6 Charles, J. P., M. Abdelkrim, Y. H. Muoy, and P. Mialhe, "A Practical Method of Analysis of the Current-Voltage Characteristics of Solar Cells," Solar Cells, 4 (1981), 169-178.

C7 Chazalviel, J.-N., "Electrochemical Transfer via Surface States: A New Formulation for the Semiconductor-Electrolyte Interface," Journal of the Electrochemical Society, 129 (1982), 963-969.

C8 Choo, Seok Cheow, "Numerical Analysis of a Forward-Biased Step-Junction p-1-n Diode," IEEE Transactions on Electron Devices, ED-18 (1971), 574-586.

C9 Choo, Seok Cheow, "Theory of a Forward-Biased Diffused-Junction p-1-n Rectifier-Part 1: Exact Numerical Solution," IEEE Transactions on Electron Devices, ED-19 (1972), 954-966.

C10 Czanderna, A. W., "Stability of Interfaces in Solar Energy Materials," Solar Energy Materials, 5 (1981), 349-377.

D1 Dare-Edwards, M. P., A. Hamnett, and J. B. Goodenough, "The Efficiency of Photogeneration of Hydrogen at P-Type III/V Semiconductors," Journal of Electroanalytical Chemistry, 119 (1981), 109-123.

D2 Dhariwal, S. R., and V. N. Ojha, "Band Gap Narrowing in Heavily Doped Solicon," Solid State Electronics, 25 (1982), 909-911.

D3 Davis, James A., Robert O. James, and James O. Leckie, "Surface Ionization and Complexation at the Oxide-Water Interface: I. Computation of Electrical Double Layer Properties in Simple Electrolytes," Journal of Colloid and Interface Science, 63 (1978), 480-499.

D4 Davis, James A., and James O. Leckie, "Surface Ionization and Complexation at the Oxide-Water Interface: II. Surface Properties of Amorphous Iron Oxyhydroxide and Adsorption of Metal Ions," Journal of Colloid and Interface Science, 67 (1978), 91-107.

D5 Davis, James A., and James O. Leckie, "Surface Ionization and Complexation at the Oxide-Water Interface: 3. Adsorption of Ions," Journal of Colloid and Interface Science, 74 (1980), 32-43.

D6 De Mari, A., "An Accurate Numerical Steady-State One-Dimensional Solution of the p-n Junction," Solid-State Electronics, 11 (1968), 33-58.

D7 De Mari, A., "An Accurate Numerical Steady-State One-Dimensional Solution of the p-n Junction under Arbitrary Transient Conditions," Solid-State Electronics, 11 (1968), 1021-1053.

D8 De Visschere, P., "A Contribution to the Theory of the Open-Circuit Photovoltage of an Abrupt p-n Junction," Solid State Electronics, 27 (1984), 131-136.

D9 De Vos, Alexis, "The Fill Factor of a Solar Cell from a Mathematical Point of View," Solar Cells, 8 (1983), 283-296.

D10 Delahay, Paul, Double Layer and Electrode Kinetics, Interscience Publishers, New York, 1965.

D11 Dewald, J. F., "Semiconductor Electrodes," Chapter 17 in Semiconductors, N. B. Hannay, editor, Reinhold Publishing Corporation, New York, 1959.

E1 Ehrenreich, H. and J. H. Martin, "Solar Photovoltaic Energy," Physics Today, 32, 9 (1979), 25-32.

E2 Ellis, Arthur B., Steven W. Kaiser, and Mark S. Wrighton, "Semiconducting Potassium Tantalate Electrodes. Photoassistance Agents for the Efficient Electrolysis of Water," Journal of Physical Chemistry, 80 (1976), 1325-1328.

E3 Ellis, Arthur B., Jeffrey M. Bolts, Steven W. Kaiser, and Mark S. Wrighton, "Study of n-Type Gallium Arsenide- and Gallium Phosphide-Based Photoelectrochemical Cells. Stabilization by Kinetic Control and Conversion of Optical Energy to Electricity," Journal of the American Chemical Society, 99 (1977), 2848-2854.

F1 Fan Fu-Ren F., Henry S. White, Bob Wheeler, and Allen J. Bard, "Semiconductor Electrodes: XXIX. High Efficiency Photoelectrochemical Solar Cells with n-WSe_2 Electrodes in an Aqueous Iodide Medium," Journal of the Electrochemical Society, 127 (1980), 518-520.

F2 Fan, Fu-Ren F., and Allen J. Bard, "Semiconductor Electrodes. 24. Behavior and Photoelectrochemical Cells Based on p-Type GaAs in Aqueous Solutions," Journal of the American Chemical Society, 102 (1980), 3677-3683.

F3 Fan, Fu-Ren F., Bob L. Wheeler, Allen J. Bard, and Rommel N. Noufi, "Semiconductor Electrodes XXXIX. Techniques for Stabilization of n-Silicon Electrodes in Aqueous Solution Photoelectrochemical Cells," Journal of the Electrochemical Society, 128 (1981), 2042-2045.

F4 Fleck, R. N., D. N. Hanson, and C. W. Tobias, "Numerical Evaluation of Current Distribution in Electrochemical Systems," Lawrence Berkeley Laboratory Report, UCRL-11612, 1964.

F5 Fonash, Stephen J., Solar Cell Device Physics, Academic Press, New York, 1981.

F6 Fornarini, L., F. Stirpe. and B, Scrosati, "Electrochemical Solar Cells with Layer-Type Semiconductor Anodes: Stabilization of the Semiconductor Electrode by Selective Polyindole Electrodeposition," Journal of the Electrochemical Society, 130 (1983), 2184-2187.

F7 Frese, Jr., Karl W., "A Study of Rearrangement Energies of Redox Species," Journal of Physical Chemistry, 85 (1981), 3911-3916.

F8 Frese, K. W., Jr., M. J. Madou, and S. R. Morrison, "Investigation of Photoelectrochemical Corrosion of Semiconductors: III. Effects of Metal Layers on the Stability of GaAs," Journal of the Electrochemical Society, 128 (1981), 1939-1943.

F9 Fujishima, Akira, and Kenichi Honda, "Electrochemical Photolysis of Water at a Semiconductor Electrode," Nature, 238 (1972), 37-38.

G1 Garrett, C. G. B., and W. H. Brattain, "Physical Theory of Semiconductor Surfaces," Physical Review, 99 (1955), 376-387.

G2 Gartner, Wolfgang W., "Depletion-Layer Photoeffects in Semiconductors," Physical Review, 116 (1959), 84-87.

G3 Gerischer, Heinz, "Semiconductor Electrode Reactions," Chapter 4 in Advances in Electrochemistry and Electrochemical Engineering, Volume 1, Paul Delahay, editor, Interscience Publishers, New York, 1961.

G4 Gerischer, Heinz, "Semiconductor Electrochemistry," chapter 5 in Physical Chemistry: An Advanced Treatise, Volume IX, H. Eyring, editor, Academic Press, New York, 1970.

G5 Gerischer, H. and J. Gobrecht, "On the Power-Characteristics of Electrochemical Solar Cells," Berichte der Bunsengesellschaft fur Physikalische Chemie, 80 (1976), 327-330.

G6 Gerischer, Heinz, "On the Stability of Semiconductor Electrodes Against Photodecomposition," Journal of Electroanalytical Chemistry, 82 (1977), 133-143.

G7 Gerischer, Heinz, "Photoelectrochemical Solar Cells," in Proceedings of the 2nd Electrochemical Photovoltaic Solar Energy Conference, R. van Overstraeten and W. Palz, editors, D. Reidel, Boston, 1979, 408-431.

G8 Gerischer, Heinz, "Heterogeneous Electrochemical Systems for Solar Energy Conversion," Pure and Applied Chemistry, 52 (1980), 2649-2667.

G9 Ginley, D. S., R. J. Baughman, and M. A. Butler, "BP-Stabilized n-Si and n-GaAs Photoanodes," Journal of the Electrochemical Society, 130 (1983), 1999-2002.

G10 Gissler, W., P. L. Lensi, and S. Pizzini, "Electrochemical Investigation of an Illuminated TiO_2 Electrode," Journal of Applied Electrochemistry, 6 (1976), 9-13.

G11 Gobrecht, J., R. Potter, R, Nottenburg, and S. Wagner, "An n-CdSe/SnO_2/n-Si Tandem Electrochemical Solar Cell," Journal of the Electrochemical Society, 130 (1983), 2280-2283.

G12 Grahame, David C., "The Electrical Double Layer and the Theory of Electrocapillarity," Chemical Reviews, 41 (1947), 441-501.

G13 Green, Mino, "Electrochemistry of the Semiconductor-Electrolyte Interface," Chapter 5 in Modern Aspects of Electrochemistry, Volume 2, J. O'M Bockris, editor, Academic Press Inc., New York, 1959.

G14 Grove, A. S., Physics and Technology of Semiconductor Devices, John Wiley and Sons, New York, 1967.

G15 Guggenheim, E. A., "The Conceptions of Electrical Potential Difference Between Two Phases and the Individual Activities of Ions," Journal of Physical Chemistry, 33 (1929), 842-849.

G16 Guy, A. G., "Calculation of Activity Coefficients of Conduction Electrons in Metals and Semiconductors," Solid State Electronics, 26 (1983), 433-436.

H1 Haak, R., and D. Tench, "Electrochemical Photocapacitance Spectroscopy Method for Characterization of Deep Levels and Interface States in Semiconductor Materials," Journal of the Electrochemical Society, 131 (1984), 275-283.

H2 Hack, M., and M. Shur, "Computer Simulation of Amorphous Silicon Based p-i-n Solar Cells," IEEE Electron Device Letters, EDL-4 (1983), 140-143.

H3 Hannay, N. B., "Semiconductor Principles," Chapter 1 in Semiconductors, N. B. Hannay, editor, Rheinhold Publishing Corporation, New York, 1959.

H4 Harris, L. A., and R. H. Wilson, "Semiconductors for Photoelectrolysis," Annual Reviews in Materials Science, 8 (1978), 99-134.

H5 Harvey, W. W., "The Relation Between the Chemical Potential of Electrons and Energy Band Parameters of the Band Theory as Applied to Semiconductors," Journal of Physics and Chemistry of Solids, 23 (1962), 1545-1548.

H6 Heller, A., K. C. Chang, and B. Miller, "Spectral Response and Efficiency Relations in Semiconductor Liquid Junction Solar Cells," Journal of the Electrochemical Society, 124 (1977), 697-700.

H7 Heller, A., B. Miller, Shirley S. Chu, and Y. T. Lee, "7.3% Efficient Thin-Film, Polycrystalline n-GaAs Semiconductor Liquid Junction Solar Cell," Journal of the American Chemical Society, 101 (1979), 7633-7634.

H8 Heller, Adam, and B. Miller, "Photoelectrochemical Solar Cells: Chemistry of the Semiconductor-Liquid Junction," Chapter 12 in Interfacial Photoprocesses: Energy Conversion and Synthesis, Advances in Chemistry Series, 184, Mark S. Wrighton, editor, American Chemical Society, Washington D. C., 1980.

H9 Heller, Adam, Barry Miller, and F. A. Thiel, "11.5 % Solar Conversion Efficiency in the Photocathodically Protected p-InP/V^{3+}-V^{2+}-HCl Semiconductor Liquid-Junction Cell," Applied Physics Letters, 38 (1981), 282-284.

H10 Heller, Adam, "Conversion of Sunlight into Electrical Power and Photoassisted Electrolysis of Water in Photoelectrochemical Cells," Accounts of Chemical Research, 14 (1981), 154-162.

H11 Heller, Adam, "Electrochemical Solar Cells," Solar Energy, 29 (1982), 153-162.

H12 Heusler, K. E., and M. Schulze, "Electron-Transfer Reactions at Semiconducting Anodic Niobium Oxide Films," Electrochimica Acta, 20 (1975), 237-244.

H13 Hirano, Katsuhiko, and Allen J. Bard, "Semiconductor Electrodes: XXVIII. Rotating Ring-Disk Electrode Studies of Photo-oxidation of Acetate and Iodide at n-TiO_2," Journal of the Electrochemical Society, 127 (1980), 1056-1059.

H14 Houston, G. J., J. F. McCann, and D. Haneman, "Optimizing the Photoelectrochemical Performance of Electrodeposited CdSe Semiconductor Electrodes," Journal of Electroanalytical Chemistry, 134 (1982), 37-47.

H15 Hovel, Harold J., "Solar Cells," Volume 11 of Semiconductors and Semimetals, R. K. Willardson and Albert C. Beer, editors, Academic Press, New York, 1975.

H16 Hovel, Harold J., "Photovoltaic Materials and Devices for Terrestrial Solar Energy Applications," Solar Energy Materials, 2 (1980), 277-312.

H17 Hwang, J. C., and J. R. Brews, "Electron Activity Coefficients in Heavily Doped Semiconductors with Small Effective Mass," Journal of Physics and Chemistry of Solids, 32 (1971), 837-845.

I1 Iles, P. A., "Evolution of Silicon Solar Cell Design," 9th IEEE Photovoltaic Specialists Conference, Silver Springs, MD, 1972, 1-5.

I2 Ioffe, A. F., Physics of Semiconductors, Academic Press Inc., New York, 1960.

J1 Johnson, E. O., "Large-Signal Surface Photovoltage Studies with Germanium," Physical Review, 111 (1958), 153-166.

J2 Johnston, Jr., W. D., H. J. Leamy, B. A. Parkinson, A. Heller, and B. Miller, "Effect of Ruthenium Ions on Grain Boundaries in Gallium Arsenide Thin Film Photovoltaic Devices," Journal of the Electrochemical Society, 127 (1980), 90-95.

J3 Josseaux, P., A. Kirsch-De Mesmaeker, J. Riga, and J. Verbist, "Improvements of CdS Film Photoanodic Behavior by Sulfur Organic Reducing Agents," Journal of the Electrochemical Society, 130 (1983), 1067-1074.

K1 Kasper, Charles, "The Theory of the Potential and the Technical Practice of Electrodeposition: I. The General Problem and the Cases of Uniform Flow," Transactions of the Electrochemical Society, 77 (1940), 353-363.

K2 Kasper, Charles, "The Theory of the Potential and the Technical Practice of Electrodeposition: II. Point-Plane and Line-Plane Systems," Transactions of the Electrochemical Society, 77 (1940), 365-384.

K3 Kasper, Charles, "The Theory of the Potential and the Technical Practice of Electrodeposition: III. Linear Polarization on Some Line-Plane Systems," Transactions of the Electrochemical Society, 78 (1940), 131-146.

K4 Kasper, Charles, "The Theory of the Potential and the Technical Practice of Electrodeposition: IV. The Flow Between and to Circular Cylinders," Transactions of the Electrochemical Society, 78 (1940), 147-161.

K5 Kasper, Charles, "The Theory of the Potential and the Technical Practice of Electrodeposition: V. The Two-Dimensional Rectangular Enclosures," Transactions of the Electrochemical Society, 82 (1942), 153-185.

K6 Kautek, W., H. Gerischer, and H. Tributsch, "The Role of Carrier Diffusion and Indirect Optical Transitions in the Photoelectrochemical Behavior of Layer Type d-Band Semiconductors," Journal of the Electrochemical Society, 127 (1980), 2471-2478.

K7 Kautek, W., and H. Gerischer, "A Kinetic Derivation of the Photovoltage for Electrochemical Solar Cells Employing Small-Band-Gap Semiconductors," Electrochimica Acta, 27 (1982), 355-358.

K8 Kazacos, M. Skyllas, and B. Miller, "Electrodeposition of CdSe Films from Selenosulfite Solution," Journal of the Electrochemical Society, 127 (1980), 2378-2381.

K9 Khan, Shahed U. M., and John O'M. Bockris, "Photoelectrochemical Kinetics and Related Devices," Chapter 3 in Modern Aspects of Electrochemistry, Volume 14, J. O'M. Bockris, B. E. Conway, and R. E. White, editors, Plenum Press, New York, 1982.

K10 Kohl, Paul A., and Allen J. Bard, "Semiconductor Electrodes: XVII. Electrochemical Behavior of n- and p-Type InP Electrodes in Acetonitrile Solutions," Journal of the Electrochemical Society, 126 (1979), 598-608.

K11 Kousik, G. S., and J. G. Fossum, "P^+-N-N^+ Solar Cells with Hole Diffusion Lengths Comparable with the Base Width: A Simple Analytic Model," Solar Cells, 5 (1981-1982), 75-79.

K12 Kumar, D. Vijay, and S. K. Sharma, "Theory of Open Circuit Photo-Voltage in Degenerate Abrupt p-n Junctions," Solid State Electronics, 25 (1982), 1161-1164.

K13 Kung, H. H., H. S. Jarrett, A. W. Sleight, and A. Ferretti, "Semiconducting Oxide Anodes in Photoassisted Electrolysis of Water," Journal of Applied Physics, 48 (1977), 2463-2469.

L1 Lamorte, M. F., and D. H. Abbott, "AlGaAs/GaAs Cascade Solar Cell Computer Modeling under High Solar Concentration," Solar Cells, 9 (1983), 311-326.

L2 Lamorte, M. F., and D. H. Abbott, "Influence of Band Gap on Cascade Solar Cell Efficiency," Solar Cells, 10 (1983), 33-48.

L3 Landsberg, P. T., Thermodynamics and Statistical Mechanics, Oxford Univ. Press, New York, 1978, p. 327.

L4 Landsberg, P. T., and S. A. Hope, "Two Formulations of Semiconductor Transport Equations," Solid-State Electronics, 20 (1977), 421-429.

L5 Landsberg, P. T., and A. G. Guy, "Activity Coefficient and the Einstein Relation," Physical Review B: Condensed Matter, 28 (1983), 1187-1188.

L6 Lanyon, H. P. D., "The Physics of Heavily Doped n^+-p Junction Solar Cells," Solar Cells, 3 (1981), 289-311.

L7 Laser, Daniel, and Allen J. Bard, "Semiconductor Electrodes: VII. Digital Simulation of Charge Injection and the Establishment of the Space Charge Region in the Absence and Presence of Surface States," Journal of the Electrochemical Society, 123 (1976), 1828-1832.

L8 Laser, Daniel, and Allen J. Bard, "Semiconductor Electrodes: VIII. Digital Simulation of Open-Circuit Photopotentials," Journal of the Electrochemical Society, 123 (1976), 1833-1837.

L9 Laser, Daniel, and Allen J. Bard, "Semiconductor Electrodes: IX. Digital Simulation of the Relaxation of Photogenerated Free Carriers and Photocurrents," Journal of the Electrochemical Society, 123 (1976), 1837-1842.

L10 Laser, Daniel, "Modes of Charge Transfer at an Illuminated Semiconductor Electrode: a Digital Simulation," Journal of the Electrochemical Society, 126 (1979), 1011-1014.

L11 Leary, D. J., J. O. Barnes, and A. G. Jordan, "Calculation of Carrier Concentration in Polycrystalline Films as a Function of Surface Acceptor State Density: Application for ZnO Gas Sensors," Journal of the Electrochemical Society, 129 (1982), 1382-1386.

L12 Lindholm, F. A., and J. G. Fossum, "Pictorial Derivation of the Influence of Degeneracy and Disorder on Nondegenerate Minority-Carrier Concentration and Recombination Current in Heavily Doped Silicon," IEEE Electron Device Letters, EDL-2 (1981), 230-234.

L13 Liu, Chin-Hsin J., Judith Olsen, David R. Saunders, and Jui H. Wang, "Photoactivation of CdSe Films for Photoelectrochemical Cells," Journal of the Electrochemical Society, 128 (1981), 1224-1228.

L14 Liu, Chin-Hsin J., and Jui H. Wang, "Spray-Pyrolyzed Thin Film CdSe Photoelectrochemical Cells," Journal of the Electrochemical Society, 129 (1982), 719-722.

L15 Loferski, Joseph J., "Theoretical Considerations Governing the Choice of the Optimum Semiconductor for Photovoltaic Solar Energy Conversion," Journal of Applied Physics, 27 (1956), 777-784.

L16 Loferski, Joseph J., "Recent Research on Photovoltaic Solar Energy Converters," Proceedings of the IEEE, 51 (1963), 667-674.

L17 Lundstrom, M. S., R. J. Schwartz, and J. L. Gray, "Transport Equations for the Analysis of Heavily Doped Semiconductor Devices," Solid-State Electronics, 24 (1981), 195-202.

M1 Macdonald, J. Ross, "Accurate Solution of an Idealized One-Carrier Metal-Semiconductor Junction Problem," Solid-State Electronics, 5 (1962), 11-37.

M2 Manassen, J., D. Cahen, and G. Hodes, "Electrochemical, Solid State, Photochemical, and Technological Aspects of Photoelectrochemical Energy Converters," Nature, 263 (1976), 97-100.

M3 Manfredotti, C., and M. Meliga, "Monte Carlo Simulation of Solar Cells," Solar Cells, 10 (1983), 211-222.

M4 Many, A., Y. Goldstein, and N. B. Grover, Semiconductor Surfaces, North-Holland Publishing Co., Amsterdam, 1965.

M5 Marshak, Alan, H., and Ritu Shrivastava, "Calculation of the Electric Field Enhancement for a Degenerate Diffusion Process," Solid State Electronics, 25 (1982), 151-153.

M6 McCann, J. F., S. P. S. Badwal, and J. Pezy, "The Electrical Analogue of an n-SnO_2-1M NaOH-Pt Cell," Journal of Electroanalytical Chemistry, 118 (1981), 115-130.

M7 McCann, J. F., and S. P. S. Badwal, "Equivalent Circuit Analysis of the Impedance Response of Semiconductor-Electrolyte-Counterelectrode Cells," Journal of the Electrochemical Society, 129 (1982), 551-559.

M8 McCann, J. F., and D. Haneman, "Recombination Effects on Current-Voltage Characteristics of Illuminated Surface Barrier Cells," Journal of the Electrochemical Society, 129 (1982), 1134-1145.

M9 McCann, J. F., S. Hinckley, and D. Haneman, "An Analysis of the Current-Voltage Characteristics of Thin-Film Front Wall Illuminated and Back Wall Illuminated Liquid Junction and Schottky Barrier Solar Cells," Journal of Electroanalytical Chemistry, 137 (1982), 17-37.

M10 Memming, R., "A Rotating Platinum-Semiconductor Ring-Disc Electrode for Analysis of Photoelectrochemical Processes," Berichte der Bunsengesellschaft fur Physikalische Chemie, 81 (1977), 732-735.

M11 Memming, R., "The Role of Energy Levels in Semiconductor-Electrolyte Solar Cells," Journal of the electrochemical Society, 125 (1978), 117-123.

M12 Memming, R., "Solar Energy Conversion by Photoelectrochemical Processes," Electrochimica Acta, 25 (1980), 77-88.

M13 Memming, R., "Charge Transfer Processes at Semiconductor Electrodes," in Electroanalytical Chemistry, Allen J. Bard, editor, Marcel Dekker, Inc., New York, 1981, 1-84.

M14 Menezes, S., A. Heller, and B. Miller, "Metal Filmed-Semiconductor Photoelectrochemical Cells," Journal of the Electrochemical Society, 127 (1980), 1268-1273.

M15 Miller, Barry, and Adam Heller, "Semiconductor Liquid Junction Solar Cells Based on Anodic Sulphide Films," Nature, 262 (1976), 680-681.

M16 Miller, B., A. Heller, M. Robbins, S. Menezes, K. C. Chang, and J. Thomson, Jr., "Solar Conversion Efficiency of Pressure-Sintered Cadmium Selenide Liquid-Junction Cells," Journal of the Electrochemical Society, 124 (1977), 1019-1021.

M17 Miller, Wesley A., and L. C. Olsen, "Model Calculations for Silicon Inversion Layer Solar Cells," Solar Cells, 8 (1983), 371-395.

M18 Mitchell, Kim W., "Status of New Thin-Film Photovoltaic Technologies," Annual Reviews in Materials Science, 12 (1982), 401-415.

M19 Moll, John L., Physics of Semiconductors, McGraw-Hill Book Company, New York, 1964.

M20 Morrison, S. R., The Chemical Physics of Surfaces, Plenum Press, New York, 1977.

M21 Morrison, S. Roy, Electrochemistry at Semiconductor and Oxidized Metal Electrodes, Plenum Press, New York, 1980.

M22 Moulton, H. Fletcher, "Current Flow in Rectangular Conductors," Proceedings of the London Mathematical Society (Ser. 2), 3 (1905), 104-110.

M23 Murr, L. E., "Interfacial Phenomena in Solar Materials," Solar Energy Materials, 5 (1981), 1-19.

N1 Nagasubramanian, G., B. L. Wheeler, and A. J. Bard, "Semiconductor Electrodes: XLIX. Evidence for Fermi Level Pinning and Surface-State Distributions from Impedance Measurements in Acetonitrile Solutions with Various Redox Couples," Journal of the Electrochemical Society, 130 (1983), 1680-1688.

N2 Nakato, Yoshihiro, Nobuyuki Takamori, and Hiroshi Tsubomura, "A Composite Semiconductor Photoanode for Water Electrolysis," Nature, 295 (1982), 312-313.

N3 Newman, John, "Numerical Solution of Coupled, Ordinary Differential Equations," Industrial and Engineering Chemistry Fundamentals, 7 (1968), 514-517.

N4 Newman, John, Electrochemical Systems, Prentice-Hall, Inc., Englewood Cliffs, New Jersey, 1973.

N5 Newman, John, "The Fundamental Principles of Current Distribution in Electrochemical Cells," in Electroanalytical Chemistry, A. J. Bard, editor, volume 6 (1973), 187-352.

N6 Noufi, Rommel, and Dennis Tench, "High Efficiency GaAs Photoanodes," Journal of the Electrochemical Society, 127 (1980), 188-190.

N7 Noufi, Rommel, Dennis Tench, and Leslie F. Warren, "Protection of n-GaAs Photoanodes with Photoelectrochemically Generated Polypyrrole Films," Journal of the Electrochemical Society, 127 (1980), 2310-2311.

N8 Noufi, Rommel, Dennis Tench, and Leslie F. Warren, "Protection of Semiconductor Photoanodes with Photoelectrochemically Generated Polypyrrole Films," Journal of the Electrochemical Society, 128 (1981), 2596-2599.

N9 Nozik, Arthur, J., "Photoelectrochemistry: Applications to Solar Energy Conversion," Annual Reviews in Physical Chemistry, 29 (1978), 189-222.

O1 Oman, Henry, and Joseph W. Gelzer, "Solar Cells and Arrays," in Energy Technology Handbook, Douglas M. Considine, editor, McGraw Hill, New York, 1977, 6.56-6.80.

O2 Omar, M. Ali, Elementary Solid State Physics: Principles and Applications, Addison-Wesley Publishing Company, Menlo Park, California, 1975.

O3 Orazem, Mark E., and John Newman, "Theoretical Analysis of Liquid-Junction Photovoltaic Cells," 159th meeting of the Electrochemical Society, Minneapolis, Minnesota, May 14, 1981.

O4 Orazem, Mark E., and John Newman, "Primary Current Distribution and Resistance of a Slotted-Electrode Cell," Journal of the Electrochemical Society, 131 (1984), 2857-2861. (LBL-15294, November, 1982.)

O5 Orazem, Mark E., Mathematical Modeling and Optimization of Liquid-Junction Photovoltaic Cells, Ph.D. dissertation, Department of Chemical Engineering, University of California, Berkeley, June 1983, LBL-16131.

O6 Orazem, Mark E., and John Newman, "Mathematical Modeling of Liquid-Junction Photovoltaic Cells: I. Governing Equations," Journal of the Electrochemical Society, 131 (1984), 2569-2574. (LBL-16210, June, 1983.)

O7 Orazem, Mark E., and John Newman, "Mathematical Modeling of Liquid-Junction Photovoltaic Cells: II. Effect of System Parameters on Current-Potential Curves," Journal of the Electrochemical Society, 131 (1984), 2574-2582. (LBL-16211, June, 1983.)

O8 Orazem, Mark E., and John Newman, "Mathematical Modeling of Liquid-Junction Photovoltaic Cells: III. Optimization of Cell Configuration," Journal of the Electrochemical Society, 131 (1984), 2582-2589. (LBL-16212, June, 1983.)

O9 Orazem, Mark E., and John Newman, "Activity Coefficients of Electrons and Holes in Semiconductors," Journal of the Electrochemical Society, 131 (1984), 2715-2717. (LBL-16786, October, 1983.)

P1 Panayotatos, P., and H. C. Card, "Recombination in the Space-Charge Region of Schottky Barrier Solar Cells," Solid State Electronics, 23 (1980), 41-47.

P2 Panish, M. B., and H. C. Casey, Jr., "The Solid Solubility Limits of Zinc in GaAs at 1000°," Journal of Physics and Chemistry of Solids, 28 (1967), 1673-1684.

P3 Panish, M. B., and H. C. Casey, Jr., "The 1040°C Solid Solubility Isotherm of Zinc in GaP: The Fermi Level as a Function of Hole Concentration," Journal of Physics and Chemistry of Solids, 28 (1968), 1719-1726.

P4 Parkinson, B. A., A. Heller, and B. Miller, "Enhanced Photoelectrochemical Solar-Energy Conversion by Gallium-Arsenide Surface Modification," Applied Physics Letters, 33 (1978), 521-523.

P5 Parkinson, Bruce, "An Evaluation of Various Configurations for Photoelectrochemical Photovoltaic Solar Cells," Solar Cells, 6 (1982), 177-189.

P6 Parsons, Roger, "Equilibrium Properties of Electrified Interphases," Chapter 3 in Modern Aspects of Electrochemistry, Volume 1, John O'M Bockris, editor, Academic Press, New York, 1954, 103-179.

P7 Pavalets, S. Yu., "Solar Converters Based on Degenerate-Semiconductor /Semiconductor P-N Heterojunctions," Geliotekhnika, 18 (1982), 3-5.

P8 Peter, L. M., "The Photoelectrochemical Properties of Anodic Cadmium Sulphide Films," Electrochimica Acta, 23 (1978), 1073-1080.

P9 Pratt, Dexter R., Margaret E. Langmuir, Robert A. Boudreau, and R. David Rauh, "Chemically Deposited CdSe Thin Films for Photoelectrochemical Cells," Journal of the Electrochemical Society, 128 (1981), 1627-1629.

R1 Radojcic, R., A. E. Hill, and M. J. Hampshire, "A Numerical Model of a Graded Band Gap CdS_xTe_{1-x} Solar Cell," Solar Cells, 4 (1980), 109-120.

R2 Rajeshwar, K., P. Singh, and J. DuBow, "Energy Conversion in Photoelectrochemical Systems: A review," Electrochimica Acta, 23 (1975), 1117-1144.

R3 Rajeshwar, K., L. Thompson, P. Singh, R. C. Kainthla, and K. L. Chopra, "Photoelectrochemical Characterization of CdSe Thin Film Anodes," Journal of the Electrochemical Society, 128 (1981), 1744-1750.

R4 Rajeshwar, K., "Charge Transfer in Photoelectrochemical Devices via Interface States: Unified Model and Comparison with Experimental Data," Journal of the Electrochemical Society, 129 (1982), 1003-1008.

R5 Rajeshwar, K., M. Kaneko, and A. Yamada, "Regenerative Photoelectrochemical Cells using Polymer-Coated n-GaAs Photoanodes in Contact with Aqueous Electrolytes," Journal of the Electrochemical Society, 130 (1983), 38-43.

R6 Reichman, J., "The Current-Voltage Characteristics of Semiconductor-Electrolyte Junction Photovoltaic Cells," Applied Physics Letters, 36 (1980), 574-577.

R7 Reichman, J., "Collection Efficiency of Low-Mobility Solar Cells," Applied Physics Letters, 38 (1981), 251-253.

R8 Reichman, Joseph, and Michael A. Russak, "Properties of CdSe Thin Films for Photoelectrochemical Cells," Journal of the Electrochemical Society, 128 (1981), 2025-2029.

R9 Reichman, J., and M. A. Russak, "Improved Efficiency of n-CdSe Thin-Film Photoelectrodes by Zinc Surface Treatment," Journal of Applied Physics, 53 (1982), 708-711.

R10 Reiss, Howard, "Photocharacteristics for Electrolyte-Semiconductor Junctions," Journal of the Electrochemical Society, 125 (1978), 937-949.

R11 Rosenberg, A. J., "Activity Coefficients of Electrons and Holes at High Concentrations," Journal of Chemical Physics, 33 (1960), 655-667.

R12 Russak, Michael A., Joseph Reichman, Horst Witzke, S. K. Deb, and S. N. Chen, "Thin Film CdSe Photoanodes for Electrochemical Photovoltaic Solar Cells," Journal of the Electrochemical Society, 127 (1980), 725-733.

S1 Sassi, G., "Variable-Gap Cells with Several Junction Energy Gaps for a High Efficiency Solar Energy System," Solar Cells, 10 (1983), 295-307.

S2 Shibib, M. Ayman, "Inclusion of Degeneracy in the Analysis of Heavily Doped Regions in Silicon Solar Cells and other Semiconductor Devices," Solar Cells, 3 (1981), 81-85.

S3 Shockley, William, and Hans J. Queisser, "Detailed Balance Limit of Efficiency of p-n Junction Solar Cells," Journal of Applied Physics, 32 (1961), 510-519.

S4 Shulman, R. G., "Recombination and Trapping," Chapter 11 in Semiconductors, N. B. Hannay, editor, Rheinhold Publishing Corporation, New York, 1959.

S5 Singal, C. M., "Analytical Expressions for the Series-Resistance-Dependant Maximum Power Point and Curve Factor for Solar Cells," Solar Cells, 3 (1981), 163-177.

S6 Singh, P., K. Rajeshwar, R. Singh, and J. DuBow, "Estimation of Series Resistance Losses and Ideal Fill Factors for Photoelectrochemical Cells," Journal of the Electrochemical Society, 128 (1981), 1396-1398.

S7 Singh, P., and J. D. Leslie, "Economic Requirements for New Materials for Solar Photovoltaic Cells," Solar Energy, 24 (1980), 589-592.

S8 Siripala, Withana, and Micha Tomkiewicz, "Surface Recombination at n-TiO_2 Electrodes in Photoelectrolytic Solar Cells," Journal of the Electrochemical Society, 130 (1983), 1062-1067.

S9 Skotheim, Terje, Ingemar Lundstrom, and Jiri Prejza, "Stabilization of n-Si Photoanodes to Surface Corrosion in Aqueous Electrolyte with a Thin Film of Polypyrrole," Journal of the Electrochemical Society, 128 (1981), 1625-1626.

S10 Skotheim, Terje, L.-G. Petersson, O. Inganas, and Ingemar Lundstrom, "Photoelectrochemical Behavior of n-Si Electrodes Protected with Pt-Polypyrrole," Journal of the Electrochemical Society, 129 (1982), 1737-1741.

S11 Smith, R. A., Semiconductors, Cambridge University Press, London, 1959.

S12 Soukup, E. J., and D. R. Slocum, "A Model for the Collection of Minority Carriers Generated in the Depletion Region of a Schottky Barrier Solar Cell," Solar Cells, 7 (1982-1983), 297-310.

S13 Sparnaay, Marcus Johannes, The Electrical Double Layer, Pergamon Press, New York, 1972.

S14 Srivastava, G. P., P. K. Bhatnagar, and S. R. Dhariwal, "Theory of Metal-Oxide-Semiconductor Solar Cells, Solid State Electronics, 22 (1979), 581-587.

S15 Srivastava, G. P., K. K. Sharma, P. K. Bhatnagar, V. N. Ojha, and S. R. Dhariwal, "Al-Si Peaked Schottky Barriers," Solar Cells, 7 (1982-1983), 209-218.

S16 Sutherland, J. E., and J. R. Hauser, "A Computer Analysis of Heterojunction and Graded Composition Solar Cells," IEEE Transactions on Electron Devices, ED-24 (1977), 363-372.

S17 Sze, S. M., Physics of Semiconductor Devices, Wiley-Interscience, New York, 1969.

T1 Tarr, N. G., and D. L. Pulfrey, "An Investigation of Dark Current and Photocurrent Superposition in Photovoltaic Devices, Solid State Electronics, 22 (1979), 265-270.

T2 Tenne, R., N. Muller, Y. Mirovsky, and D. Lando, "The Relation Between Performance and Stability of Cd-Chalcogenide/Polysulfide Photoelectrochemical Cells: I. Model and the Effect of Photoetching," Journal of the Electrochemical Society, 130 (1983), 852-860.

T3 Tomkiewicz, M., and H. Fay, "Photoelectrolysis of Water with Semiconductors," Applied Physics, 18 (1979), 1-28.

T4 Tsou, C. C., and J. R. Cleveland, "Polycrystalline Thin-Film CdSe Liquid Junction Photovoltaic Cell," Journal of Applied Physics, 51 (1980), 455-458.

U1 Uosaki, Kohei, and Hideaki Kita, "Effects of the Helmholtz Layer Capacitance on the Potential Distribution at Semiconductor/Electrolyte Interface and the Linearity of the Mott-Schottky Plot," Journal of the Electrochemical Society, 130 (1983), 895-897.

U2 Uosaki, Kohei, and Hideaki Kita, "Photoelectrochemical Characteristics of Semiconductor-Metal/SPE/Metal Cells," Journal of the Electrochemical Society, 130 (1983), 2179-2184.

V1 Van Vliet, Karel, M., and Alan H. Marshak, "The Shottky-Like Equations for the Carrier Densities and the Current Flows in Materials with a Nonuniform Composition," Solid State Electronics, 23 (1980), 49-53.

V2 Vanden Berghe, R. A. L., W. P. Gomes, and F. Cardon, "Some Aspects of the Anodic Behavior of CdS Single Crystals in Indifferent Electrolyte Solutions," Berichte der Bunsengesellschaft fur Physikalische Chemie, 77 (1973), 289-293.

W1 Wagner, Sigurd, "Physico-Chemical Problems in Photovoltaic Research," Berichte der Bunsengesellschaft fur Physikalische Chemie, 84 (1980), 991-995.

W2 Weaver, N. L., R. Singh, K. Rajeschwar, P. Singh, and J. DuBow, "Economic Analysis of Photoelectrochemical Cells," Solar Cells, 3 (1981), 221-232.

W3 White, Henry S., Hector D. Abruna, and Allen J. Bard, "Semiconductor Electrodes XLI. Improvement of Performance of n-WSe_2 Electrodes by Electrochemical Polymerization of o-Phenylenediamine at Surface Imperfections," Journal of the Electrochemical Society, 129 (1982), 265-271.

W4 White, Ralph Edward, Simultaneous Reactions on a Rotating-Disk Electrode, PhD thesis, University of California, Berkeley, March 1977 (LBL-6094).

W5 White, Ralph, Charles M. Mohr, Jr., Peter Fedkiw, and John Newman, "The Fluid Motion Generated by a Rotating Disk: A Comparison of Solution Techniques," Lawrence Berkeley Laboratory Report, LBL-3910, November 1975.

W6 Williams, Fred, and A. J. Nozik, "Irreversibilities in the Mechanism of Photoelectrolysis," Nature, 271 (1978), 137-139.

W7 Williams, Larry McClease, Structural and Photoelectrochemical Properties of Plasma Deposited Titanium Dioxide, PhD thesis, University of California, Berkeley, December, 1982 (LBL-14994).

W8 Wilson, Ronald H., "A Model for the Current-Voltage Curve of Photoexcited Semiconductor Electrodes," Journal of Applied Physics, 48 (1977), 4292-4297.

W9 Wilson, Ronald H., "A Model for the Current-Voltage Curve of Photoexcited Semiconductor Electrodes," Semiconductor Liquid-Junction Solar Cells, Adam Heller, editor, The Electrochemical Society, Princeton, N.J., 1977.

W10 Wilson, R.H., "Electron Transfer Processes at the Semiconductor-Electrolyte Interface," CRC Critical Reviews in Solid State and Materials Science, 10 (1980), 1-41.

W11 Wilson, R. H., "Observation and Analysis of Surface States on TiO_2 Electrodes in Aqueous Electrolytes," Journal of the ELectrochemical Society, 127 (1980), 228-234.

W12 Wolf, M., "Limitations and Possibilities for Improvement of Photovoltaic Solar Energy Converters, Part I: Considerations for Earth's Surface Operation," Proceedings of the IRE, 48 (1960), 1246-1263.

W13 Wrighton, Mark S., Jeffrey M. Bolts, Andrew B. Bocarsly, Michael C. Palazzotto, and Erick G. Walton, "Stabilization of n-Type Semiconductors to Photoanodic Dissolution: II-VI and III-V Compound Semiconductors and Recent Results for n-Type Silicon," Journal of Vacuum Science Technology, 15 (1978), 1429-1435.

W14 Wrighton, Mark S., "Photoelectrochemical Conversion of Optical Energy to Electricity and Fuels," Accounts of Chemical Research, 12 (1979), 303-310.

W15 Wysocki, J. J., "Photon Spectrum Outside the Earth's Atmosphere," Solar Energy, 6 (1962), 104.

7. Figure Captions

Figure 1. The photoelectrochemical cell.

Figure 2. Physical model of the semiconductor-electrolyte interface in a photoelectrochemical cell.

Figure 3. Potential distribution for the photoelectrochemical cell with no interfacial kinetic limitations. Curve a, open circuit in the dark; curve b, open circuit under 882 W/m^2 illumination; and curve c, near short circuit ($\underline{i}$ = -23.1 mA/cm^2) under illumination.

Figure 4. Concentration distribution for the photoelectrochemical cell with no interfacial kinetic limitations. Curve a, open circuit in the dark; curve b, open circuit under 882 W/m^2 illumination; and curve c, near short circuit ($\underline{i}$ = -23.1 mA/cm^2) under illumination. Concentrations are dimensionalized by the net dopant concentration N_d-N_a.

Figure 5. Schematic representation of band-to-band recombination kinetics in the semiconductor.

Figure 6. Schematic representation of single-trap recombination kinetics in the semiconductor.

Figure 7. Slotted-electrode photoelectrochemical cell; (a) three-dimensional configuration, (b) two-dimensional representation, and (c) repeating section.

Figure 8. Primary resistance of a slotted-electrode cell as a function of L/h.

Figure 9. Maximum power density as a function of L/h for the slotted-electrode photoelectrochemical cell.

Figure 10. Maximum power efficiency as a function of the fraction of peak AM-2 illumination for a slotted-electrode photoelectrochemical cell with h/G=10 and L/h=0.5.

Figure 11. Cell potential as a function of current density for (a) a front-illuminated semiconductor without kinetic, electrolyte resistance, and counterelectrode limitations; (b) an optimally designed slotted-electrode cell with a porous counterelectrode; and (c) an optimally designed cell with a wire-grid counterelectrode of radius 0.5 cm.

This report was done with support from the Department of Energy. Any conclusions or opinions expressed in this report represent solely those of the author(s) and not necessarily those of The Regents of the University of California, the Lawrence Berkeley Laboratory or the Department of Energy.

Reference to a company or product name does not imply approval or recommendation of the product by the University of California or the U.S. Department of Energy to the exclusion of others that may be suitable.

TECHNICAL INFORMATION DEPARTMENT
LAWRENCE BERKELEY LABORATORY
UNIVERSITY OF CALIFORNIA
BERKELEY, CALIFORNIA 94720